

Scientific Inquiry and Review (SIR)

Volume 7 Issue 4, 2023

ISSN (P): 2521-2427, ISSN (E): 2521-2435

Homepage: <https://journals.umt.edu.pk/index.php/SIR>



Article QR



- Title:** Plant-Extract of *Mimusops elengi* leaves and Flower-Mediated ZnO Nanoparticles: Synthesis, Characterization, and Biomedical Applications
- Author (s):** Iram Bashir, Syeda Shaista Gillani*, and Fouzia Majeed
- Affiliation (s):** Department of Chemistry, Lahore Garrison University, Pakistan
- DOI:** <https://doi.org/10.32350/sir.74.01>
- History:** Received: May 31, 2023, Revised: September 11, 2023, Accepted: September 12, 2023, Published: 27 October, 2023
- Citation:** Bashir I, Gillani SS, Majeed F. Plant-Extract of *Mimusops elengi* leaves and Flower-Mediated ZnO Nanoparticles: Synthesis, Characterization, and Biomedical Applications. *Sci Inq Rev.* 2023;7(4):1–18. <https://doi.org/10.32350/sir.74.01>
- Copyright:** © The Authors
- Licensing:**  This article is open access and is distributed under the terms of [Creative Commons Attribution 4.0 International License](https://creativecommons.org/licenses/by/4.0/)
- Conflict of Interest:** Author(s) declared no conflict of interest



A publication of
The School of Science
University of Management and Technology, Lahore, Pakistan

Plant-Extract of *Mimusops elengi* leaves and Flower-Mediated ZnO Nanoparticles: Synthesis, Characterization, and Biomedical Applications

Iram Bashir, Syeda Shaista Gillani*, and Fouzia Majeed

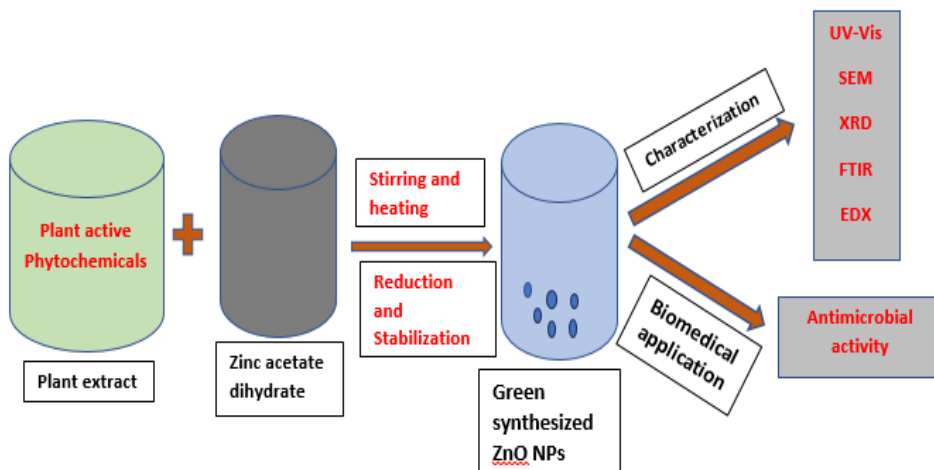
Department of Chemistry, Lahore Garrison University, Pakistan

ABSTRACT

The current study aims to employ an ecologically sustainable method, utilizing a plant-based extract derived from *Mimusops elengi* as both a reducing and capping agent. Synthesis of zinc oxide nanoparticles (ZnO NPs) was done from aqueous leaves and flower extracts of *Mimusops elengi*. Different spectroscopic techniques were used to characterize these biosynthesized (ZnO NPs) zinc oxide nanoparticles like UV-visible, FTIR, XRD, SEM, and EDX techniques. UV-visible spectroscopy showed the absorption wavelength of ZnO NPs at 353nm (leaves extracts) and 365nm (flowers extracts). FTIR spectra showed the absorption frequency of different functional groups present in plant extract along with ZnO peak at 637cm^{-1} (leaves extracts) and 643cm^{-1} (flowers extracts). XRD results revealed the hexagonal structure and crystalline nature of biosynthesized ZnO NPs. The average grain size calculated for ZnO NPs of leaves and flower extracts was 10.37 and 15.52nm, respectively. SEM analysis showed a hexagonal shape. EDX confirmed the formation and purity of ZnO NPs by showing an abundant % of zinc and oxygen atoms. The significant bactericidal efficacy of biosynthesized ZnO NPs was found against pathogens *Escherichia coli* and *Staphylococcus aureus*. When compared to ZnO nanoparticles from flower extracts and biosynthesized ZnO nanoparticles from leaf extract exhibited substantial suppression. ZnO-NPs synthesized from leaves and flower extracts of *Mimusops elengi* can be subjugated for biomedical and ecologically sustainable applications.

* Corresponding Author: shaistaaligillani@gmail.com

Graphical Abstract



Keywords: antibacterial, biomedical, green synthesis, *Mimusops elengi*, nanoparticles (NPs)

1. INTRODUCTION

In 1959, at the California Institute of Technology (Caltech), a Nobel Laureate, Richard Feynman presented a notable speech during a conference hosted by the American Physical Society titled: *There's Plenty of Space at the bottom* [1], in which he explored the groundbreaking concept of nanotechnology and the potential for crafting intricate molecular machines with atomic accuracy. Nanotechnology is the atomic-scale manipulation of matter and has applications in various fields. Nanoparticles (NPs) are microscopic particles made up of both organic and inorganic materials [2]. Due to their tiny size (1-100 nm), high energy at the surface, and larger (S/V) surface area to volume ratio, their catalytic capabilities and interaction with other molecules increased, significantly [3].

In the last decade, comprehensive research concerning metal oxide nanoparticles has been emphasized due to their myriad applications in several technology sectors. Zinc Oxide (ZnO NPs) is one of the materials in nature that show great diversity in the structure, of all known materials and is an interesting inorganic material with several advantages in current laser medical, biomedical, and optoelectronic technology [4–7]. ZnO NPs are categorized as a semiconductor in material science because of their covalent and ionic bonds. Due to a large energy band (3.37 MeV) and broad energy

bond (60MeV), ZnO NPs have captivated a lot of consideration because of their high mechanical capabilities and thermal stability at ambient temperature. ZnO NPs are more appealing and effective in current laser medical technology, electronics, and optoelectronic technology because of this significant characteristic [5].



Figure 1. Some Appealing Properties of Zinc Oxide Nanoparticles

Zinc Oxide nanomaterials possess a range of structures, which act as a novel material and have potential uses in a number of nanotechnology sectors. These particles have showed the potential to photo-oxidize and photo-catalyze chemical reactions and biological species, as a result of this ability, they are a key player in cancer therapy [8].

ZnO is one of five chemicals that are classified as "generally regarded as safe". ZnO has been widely utilized in cosmetics, sunscreens, lotions, medication delivery, and bio-imaging due to its bio safe and biocompatible characteristics [3]. ZnO NPs have been explored as an antibacterial and anticancer agent in several other research investigations [7].

Several techniques are reported for the synthesis of nanoparticles, which are classified into three types: Physical (mechanical), chemical, and biological [9]. Green synthesis is a relatively recent phrase that refers to the employment of ecologically sustainable methods for the creation of new products that do not affect the environment. In physical and chemical methods dangerous substances are being absorbed on the surface [10].

As physical and chemical procedures became more expensive day by day, the necessity for biosynthesis of nanoparticles emerged as a new trend. Chemical synthesis processes usually result in dangerous substances being absorbed on the surface, which may have negative consequences in clinical uses [11, 12]. In order to find cost-effective ways to make nanoparticles, scientists turned to microbial enzymes and plant extracts (phytochemicals), which are generally responsible for the reduction of metals into their respective nanoparticles, due to their antioxidant or reducing capabilities. Green synthesis is less expensive, more eco conscious, and simpler for high yield production than chemical or physical synthesis as it does not need the use of high pressure, power, temperature, or dangerous substances.

The current study focused on the leaves and flowers of *Mimusops elengi* Linn. (*M. elengi*), which is a fragrant ornamental tree belonging to the Sapotaceae family. Hindus regard *Mimusops elengi* as a holy plant and a symbol of love and beauty [13]. The bark of *Mimusops elengi* is used as a cooling agent, a cardi tonic, the blossoms are used to treat asthma, and are smoked [14]. The fruit of *Mimusops elengi* is edible; it has astringent properties, is excellent for the teeth and produces flatulence, the seed is used to repair loose teeth and to treat headaches [15]. The phytochemicals present in the aqueous extract of *Mimusops elengi*, functions as an oxidizing, reducing, and stabilizing agent for the biosynthesis of these zinc oxide nanoparticles (ZnO NPs).

2. MATERIALS AND METHOD

Chemicals: Zinc acetate dihydrate [$\text{Zn}(\text{C}_2\text{H}_3\text{O}_2)_2 \cdot 2\text{H}_2\text{O}$] and sodium hydroxide (NaOH) were purchased from Sigma-Aldrich

All of the reagents and solvents used for this research work were of excellent analytical quality and purchased from Sigma-Aldrich. Solvents were refined by distillation before usage. The leaves and flowers of *Mimusops elengi* were collected from Baagh-e-Jinnah, Lahore, Pakistan.

2.1. Aqueous Extraction of Leaves and Flowers of *Mimusops elengi*

Freshly collected leaves and flowers of *Mimusops elengi* were scrupulously washed with water to remove debris on the surface and then rinsed with distilled water. After that, leaves and flowers were shade-dried for a week, weighed (12g), and crushed to a fine powder, separately. Then, the powder of leaves and flowers was mixed and heated with 100 mL distilled water at 20°C for an hour, while swirling constantly with vigorous

stirring, separately. The mixtures were filtered twice, first with muslin cloth and once with Whatman No. 1 filter paper, separately. Dark green extracts (leaves) and pale orange extracts (flowers) were obtained and stored at 4 °C for further processing.

2.2. Preparation of Salt Solution

5.48g of zinc acetate dihydrate was dissolved in 100 mL of distilled water to produce 0.25M zinc acetate dihydrate ($\text{Zn}(\text{C}_2\text{H}_3\text{O}_2)_2 \cdot 2\text{H}_2\text{O}$) solution.

2.3. Green Synthesis of Zinc Oxide Nanoparticles

A 100 mL of 0.25M zinc acetate dihydrate ($\text{Zn}(\text{C}_2\text{H}_3\text{O}_2)_2 \cdot 2\text{H}_2\text{O}$) solution was mixed with 50 mL leaves extract and 50 mL flowers extract in a 250 mL flask, separately. The colour of the mixture changed from dark green to brown for the leaves and pale orange to brown for the flower extracts after 1 hour of incubation at 40°C with continual shaking, suggesting that green manufactured zinc oxide nanoparticles had been generated. Then 0.02 M NaOH was added drop by drop to keep the pH of the solution at 12. As a result, bio-reduced salt sank to the flask's bottom. After that, the sample was washed with distilled water before being exposed to ethanol. The washing procedure was repeated three times to ensure that all contaminants were eliminated. The washed ZnO NPs were then oven-dried for 24 hours at 60°C. The powdered ZnO NPs were then kept for future analysis.

2.4. Antibacterial Assay

The antibacterial activity of biosynthesized ZnO nanoparticles was tested using two bacterium strains. The antibacterial activity was measured using the Agar well diffusion method. The antibacterial activity of biologically produced zinc oxide (ZnO) nanoparticles against gram-positive (*Staphylococcus aureus*) and gram-negative (*Escherichia coli*) bacterial strains was tested. Three wells were made on each agar plate, added 10 µL ZnO NPs, Ciprofloxacin (standard reference), and left it for 24 hours.

3. RESULTS AND DISCUSSION

3.1. Characterization Techniques

UV- Visible Spectroscopy (Ultra-3000), Fourier transforms infrared (FTIR) spectroscopy, X-ray Diffraction (XRD) (Bruker AXS D8), Scanning

Electron Microscopy (SEM) (HITECH-3400-N), and Energy dispersive X-ray (EDX) analysis was used to characterize the synthesized zinc oxide nanoparticles (ZnO NPs).

3.2. UV-Visible

The UV-visible spectra were recorded on an Ultra 3000 UV-Vis spectrophotometer for these green synthesized ZnO NPs. The spectrophotometer was allowed to scan at wavelength ranges from 200-800nm. The λ_{max} at 353 nm (a) and 365 nm (b) [16] depicts the Surface Plasmon Resonance (SPR) phenomena when the ground state non-bonding electrons excited to a higher energy state [17, 18], as a result, a change in colour was noticed from dark green to brown, while the colour of the flower extract changed from pale orange to light brown. The monodispersed character of NPs distribution is confirmed by the strong absorption peaks of ZnO.

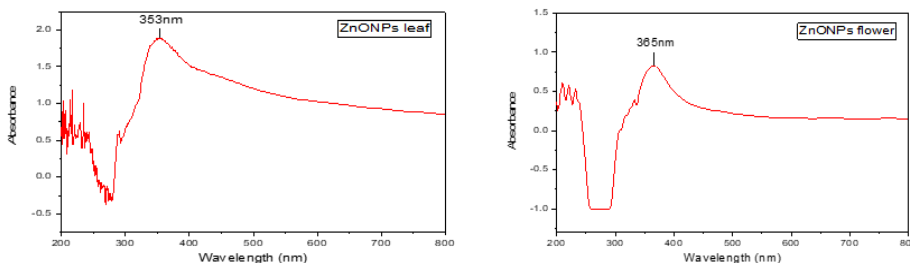


Figure 2. UV-Vis Spectra: (a) Zn ONPs for Leaves Extract and (b) Zn ONPs for Flower Extract

3.2.1. Fourier Transforms Infrared (FTIR). Fourier transforms infrared spectroscopy ($4000\text{--}400\text{ cm}^{-1}$) was used to categorize functional groups in aqueous extract and zinc oxide nanoparticles (ZnO NPs). (FTIR) spectrum of biosynthesized Zn ONPs was used for the leaf extract, which is given in Figure 3. By using the FTIR technique, the phytochemical composition of biomolecules resulted in the reduction and stability of ZnO NPs. The broad peak at 3085 cm^{-1} links to the OH [19] group of carboxylic acid along with C=O stretching at 1560 cm^{-1} [20]. The peak at 1560 cm^{-1} may also be due to the N-H bending of alkaloids or the N=O group showing asymmetric stretching vibrations. The peak at 2313 cm^{-1} resulted from =C-H stretch of aromatic aldehyde. The sharp peak at 1408 cm^{-1} showed symmetric stretching of the N=O bond or C-N stretch and the peak at

1014cm^{-1} was because of C-O stretching vibration [21], which represent acidic, alcoholic, phenolic, and aromatic nitro compounds. The fingerprint region of the spectrum contained a peak at 637cm^{-1} confirming the presence of Zn-O. Previous literature has reported, the range of $400\text{-}500\text{ cm}^{-1}$ for the absorption bands [22] or for higher frequencies, however, $608\text{-}731\text{ cm}^{-1}$ [23] were indicated for the distinctive peaks for ZnO vibrations.

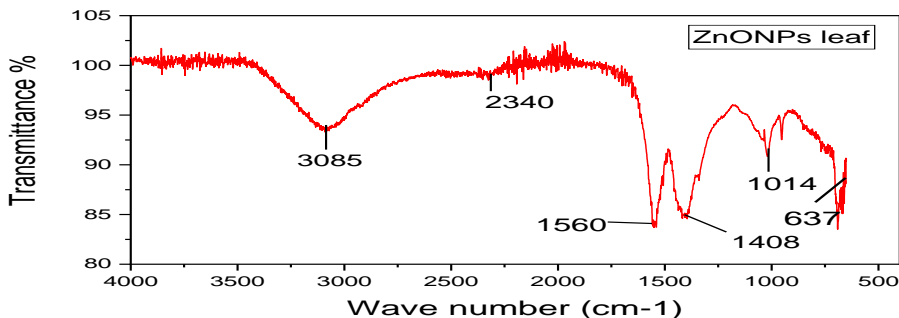


Figure 3. FTIR Spectrum of ZnO NPs (leaves Extract)

Figure 4 shows the IR spectrum of zinc oxide nanoparticles for the flower extract. It showed some characteristic peaks, which were observed because phytochemicals exist in extract and are accountable for nanoparticle fabrication and maintenance. The broad peak at 3120cm^{-1} was because of the phenolic or alcoholic hydroxyl (OH) group. A small peak at 2868cm^{-1} resulted from $-\text{CH}$ stretching frequency. The high-pitched peak at 1609cm^{-1} was observed due to carbonyl stretch, aromatic $\text{C}=\text{C}$ stretching, or N-H bending vibrations. Another sharp peak at 1326cm^{-1} showed the presence of the C-N group as well as the amide band of proteins [24]. The medium-strong peak at 1103cm^{-1} links to a stretch of the C-O bond. The signal at 643cm^{-1} was caused by a Zn-O link, indicating that zinc oxide nanoparticles were synthesized [23].

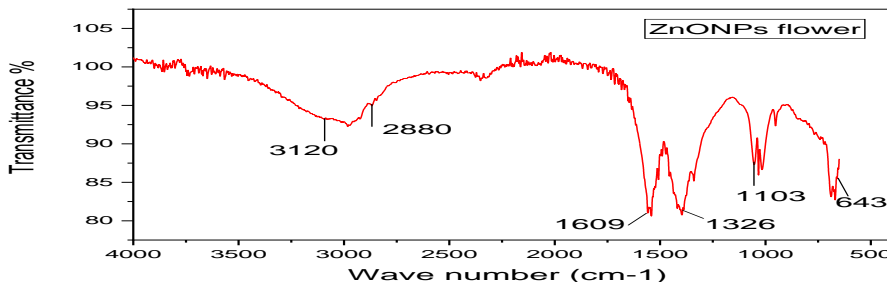


Figure 4. FTIR Spectrum of ZnO NPs (Flowers Extract)

3.2.2. X-ray Diffraction. XRD examination was done to evaluate the crystallographic nature and phase purity of these biosynthesized zinc oxide nanoparticles (see Figure 5). The XRD peaks of ZnO NPs for the leaves extract diffracted at 2θ angle are 31.63° , 34.31° , 37.12° , 47.80° , 57.68° , 63.52° , and 68.84° that showed 100, 002, 101, 102, 110, 103, and 112 Miller indexes planes, respectively. The obtained peaks were consistent with those reported in [25]. The hexagonal wurtzite structure of zinc oxide nanoparticles is represented by all sample's diffraction peaks. Planes of hexagonal ZnO nanoparticles significantly matched with standard card values (JCPDS PDF No 36-1451). The size of the crystalline nanoparticles was enumerated by using the Debye–Scherrer formula [25, 26].

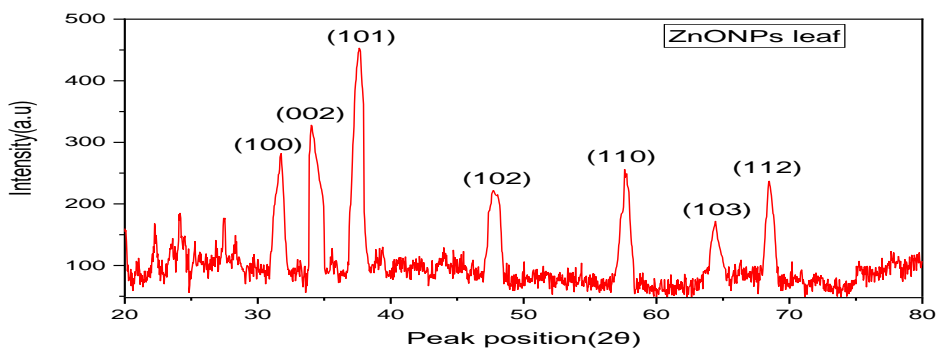


Figure 5. XRD Graph of ZnO NPs (Leaves Extracts)

The X-ray diffraction peaks of green synthesized zinc oxide nanoparticles for the flower extract given in Figure 6 at 2θ diffracted angle are 32.93° , 34.70° , 37.68° , 49.25° , 57.67° , 63.86° , and 69.98° exhibiting 100, 002, 101, 102, 110, 103, and 201 Miller indexes planes, respectively. The Peak search approach was used to compare the peak pattern with the previously reported patterns (found in the library), confirming that the synthesized product has a hexagonal structure due to its distinctive pattern. The crystalline nature of ZnO NPs was revealed by the strong peaks. The single-phase purity of the ZnO NPs is also shown by the placement and sharpness of the peaks [27]. The obtained peaks were consistent with those reported in [25]. The average size calculated was 15.52 nm (Debye Scherrer equation).

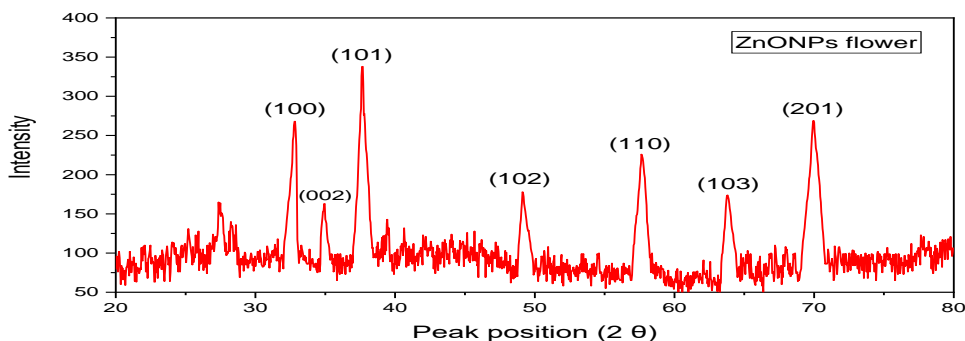


Figure 6. XRD Graph of ZnO NPs (Flowers Extracts)

3.2.3. Scanning Electron Microscopy (SEM). The surface morphology of ZnO NPs from leaves and flower extracts was hexagonal wurtzite (see Figure 7). The average grain size calculated for ZnO NPs of leaves and flower extracts was 10.37 and 15.52nm, respectively. SEM analysis showed a hexagonal shape. Altered forms of ZnO NPs have previously been observed, with sphere-shaped, hexagonal, and flower-like shapes being the most prevalent among them [28, 29].

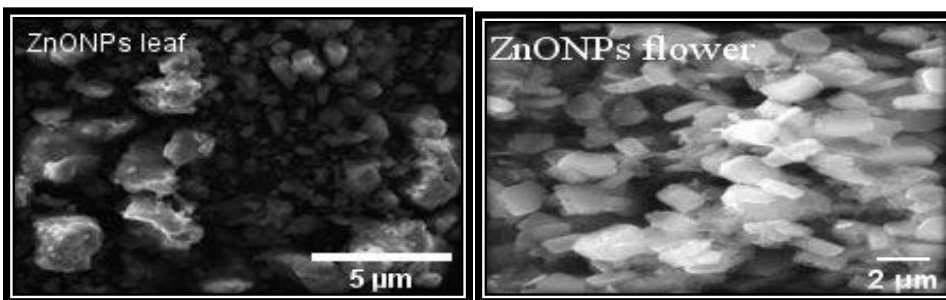


Figure 7. SEM Images of ZnONPs Leaves and Flowers Extracts

3.2.4. Energy Dispersive X-ray (EDX). This technique was utilized to recognize different types of elements present in the selected sample. This study revealed that the current sample contains a significant amount of zinc (52.94% in the leaf and 50.96% in the flower) and oxygen (40.94% in the leaf and 40.08% in the flower) with a trace amount of C, Pb, K, Cl, and P elements. The trace elements may come from the soil and environment of the plant. The elemental distribution of the ZnO NPs was confirmed by the EDX spectra, which indicated the main peaks between 0.5-8.5 keV [30]. The purity of zinc oxide nanoparticles (ZnO NPs) was revealed [31] with high Zn and oxygen element composition and the synthesis of ZnO NPs was

confirmed. The purity of ZnO NPs from the leaf was 93.88% (40.94%+52.94%) and 91.04% (40.08%+50.96%) for the flower ZnO NPs.

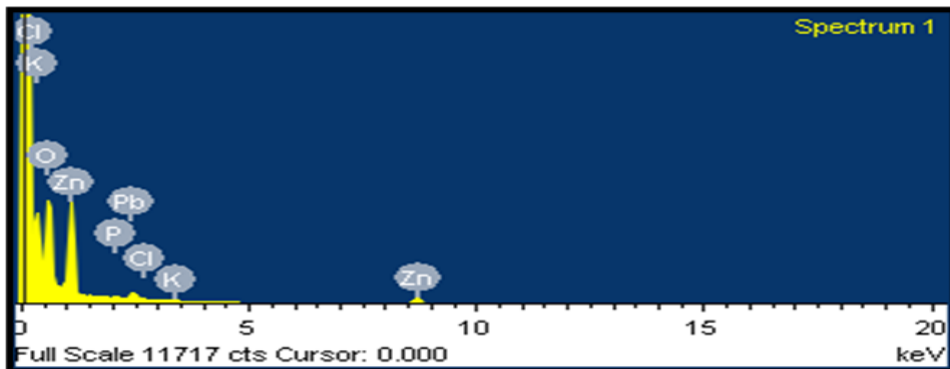


Figure 8. EDX Spectrum of ZnO NPs (Leaves Extracts)

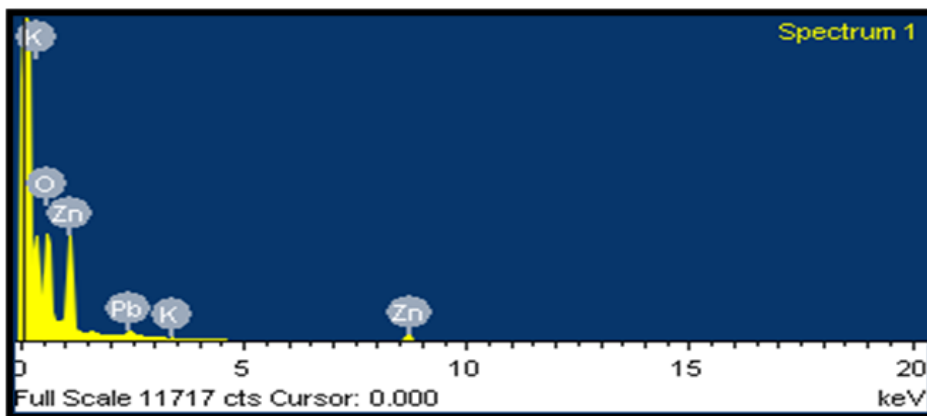


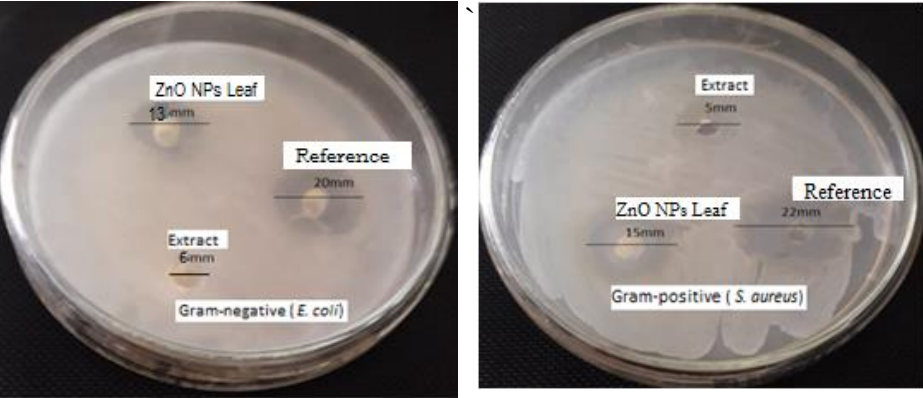
Figure 9. EDX Spectrum of ZnO NPs (Flowers Extracts)

3.3. Measurement of Antibacterial Activity

Biosynthesized zinc oxide nanoparticles from leaves have antibacterial action against pathogens of importance (see Figure 10). The antibacterial activity of ZnO NPs from the leaves at 100 μ g/mL concentration was 13mm, leaves extract showed 6mm, while the reference (Ciprofloxacin) was measured at 20mm zone of inhibition against *E.coli* (Gram-negative) bacteria. Also, *S.aureus* (Gram-positive) bacteria showed 15mm for ZnO NPs, 5mm for leaves, and 22mm zones of inhibition against the reference.

Inhibition zones of zinc oxide nanoparticles (ZnO NPs) produced from *Mimusops elengi* flowers were equally impressive (see Figure 12). Against

E.coli, the ZOI for floral ZnO NPs was 10mm, 15mm for the reference, and 3mm for the flower extract. Additionally, the ZOI against *S. aureus* was measured at 16mm for ZnO NPs 20mm for reference, and 8mm for flowers extract. As the size of ZnO NPs from the leaves is less as compared to ZnO NPs from the flowers, it showed a greater antibacterial effect. Nanoparticles' antibacterial activity is a size-dependent on the characteristics, which gradually improves when the particle size is reduced [32].



Gram-negative *Escherichia coli* Gram-positive *Staphylococcus aureus*

Figure 10. Zone of Inhibitions by Zn ONPs (Leaves Extract)

Table 1. Measured ZOI against *E.coli* and *S.aureus*

Clinical pathogenic strains	ZOI (mm)		
	Leaves extract	ZnO NPs (Leaves extracts)	Reference (Ciprofloxacin)
(a) <i>Escherichia coli</i>	6mm	13mm	20mm
(b) <i>Staphylococcus aureus</i>	5mm	15mm	22mm

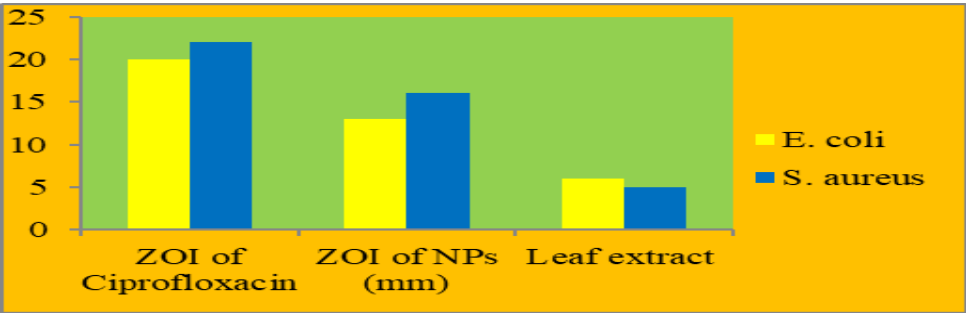
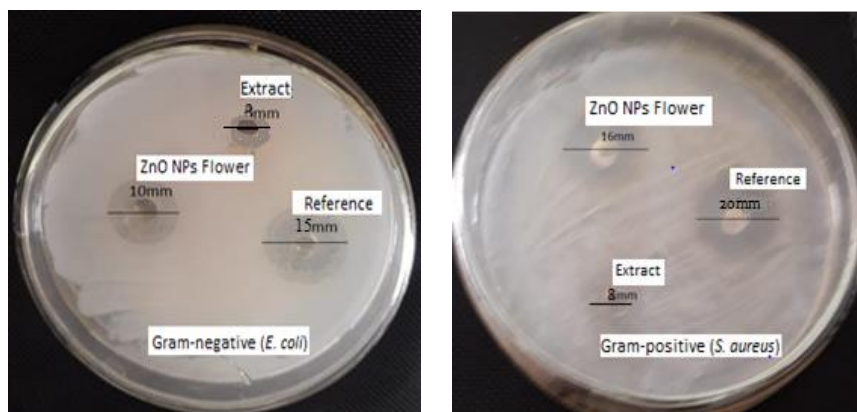


Figure 11. Bar Graph for the Measured Zone of Inhibition



Gram-negative *Escherichia coli* Gram-positive *Staphylococcus aureus*

Figure 12. Zone of Inhibition by ZnO NPs (Flowers Extract)

Table 2. Measured Zones of Inhibition of ZnO NPs from Flower

Clinical pathogenic strains	Zone of Inhibition (ZOI) (mm)		
	Flowers extract	ZnO NPs (Flowers extract)	Reference (Ciprofloxacin)
(a) <i>Escherichia coli</i>	3mm	10 mm	15mm
(b) <i>Staphylococcus aureus</i>	8 mm	16 mm	20mm

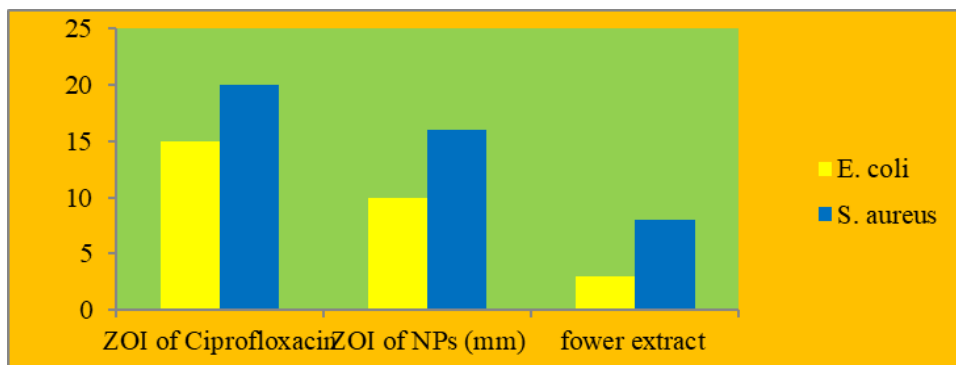


Figure 13. Bar Graph Representing the ZOI against *E.coli* and *S.aureus*

The presence of an inhibitory zone indicates that ZnO nanoparticles' biocidal action involves membrane rupture with a greater rate of surface oxygen species, which results in pathogen loss. ZnO nanoparticles produced from *Mimusops elengi* leaves and flower extract exhibit antibacterial

properties. According to the findings, ZnO nanoparticles were made from *Mimusops elengi* leaf and flower extract against *E.coli* and *S.aureus*. In comparison to ZnO nanoparticles (flowers), biosynthesized ZnO nanoparticles (leaves) exhibited substantial suppression [33].

4. CONCLUSION

Conclusively, this study provided a convenient and cost-effective method to synthesize ZnO NPs by using *Mimusops elengi* as a novel reducing and stabilizing agent. The ZnO NPs were characterized by SEM, UV–Vis, FTIR, XRD, and EDX spectroscopy. UV-visible spectroscopy showed the maxima absorption of ZnO NPs at 353nm (leaves extracts) and 365nm (flowers extracts). FTIR spectra showed the absorption frequency of different functional groups present in plant extract along with ZnO peak at 637cm⁻¹ (leaves extracts) and 643cm⁻¹ (flowers extracts). XRD results revealed the hexagonal structure and crystalline nature of biosynthesized ZnO NPs. The average grain size calculated for ZnO NPs of leaves and flower extracts was 10.37 and 15.52nm, respectively. SEM analysis showed a hexagonal shape. EDX confirmed the formation and purity of ZnO NPs by showing an ample % of zinc and oxygen atoms. ZnO NPs showed significant antibacterial activity against clinical pathogens *Escherichia coli* and *Staphylococcus aureus*. ZnO NPs synthesized from flowers showed a higher bactericidal impact on the tested pathogens in comparison to ZnO NPs synthesized, which was synthesized from leaves. Certainly, green - synthesized zinc oxide nanoparticles (ZnO NPs) were ecologically sustainable, and can be employed in various biological applications.

REFERENCES

1. Treguer M, De Cointet C, Remita H, et al. Dose rate effects on radiolytic synthesis of gold– silver bimetallic clusters in solution. *J Phys Chem.* 1998;102(22):4310–4321. <https://doi.org/10.1021/jp981467n>
2. LaConte L, Nitin N, Bao G. Magnetic nanoparticle probes. *Mater Today.* 2005;8(5):32–38. [https://doi.org/10.1016/S1369-7021\(05\)00893-X](https://doi.org/10.1016/S1369-7021(05)00893-X)
3. Iqbal J, Abbasi BA, Mahmood T, Hameed S, Munir A, Kanwal S. Green synthesis and characterizations of Nickel oxide nanoparticles using leaf extract of *Rhamnus virgata* and their potential biological applications. *Appl Organomet Chem.* 2019;33(8):e4950. <https://doi.org/10.1002/aoc.4950>

4. Altavilla C, Ciliberto E. *Inorganic Nanoparticles: Synthesis, Applications, and Perspectives*. CRC Press; 2017.
5. Wang J, Cao J, Fang B, Lu P, Deng S, Wang H. Synthesis and characterization of multipod, flower-like, and shuttle-like ZnO frameworks in ionic liquids. *Mat Lett*. 2005;59(11):1405–1408. <https://doi.org/10.1016/j.matlet.2004.11.062>
6. Bacaksiz E, Parlak M, Tomakin M, Özçelik A, Karakız M, Altunbaş M. The effects of zinc nitrate, zinc acetate and zinc chloride precursors on investigation of structural and optical properties of ZnO thin films. *J Alloys Comp*. 2008;466(1-2):447–450. <https://doi.org/10.1016/j.jallcom.2007.11.061>
7. Abbasi BA, Iqbal J, Mahmood T, Qyyum A, Kanwal S. Biofabrication of iron oxide nanoparticles by leaf extract of *Rhamnus virgata*: characterization and evaluation of cytotoxic, antimicrobial and antioxidant potentials. *Appl Organomet Chem*. 2019;33(7):e4947. <https://doi.org/10.1002/aoc.4947>
8. Zhang H, Chen B, Jiang H, Wang C, Wang H, Wang X. A strategy for ZnO nanorod mediated multi-mode cancer treatment. *Biomaterials*. 2011;32(7):1906–1914. <https://doi.org/10.1016/j.biomaterials.2010.11.027>
9. Iravani S, Korbekandi H, Mirmohammadi SV, Zolfaghari B. Synthesis of silver nanoparticles: chemical, physical and biological methods. *Res Pharm Sci*. 2014;9(6):385–406.
10. De Melo CG, Pereira LHDS, Da Costa LAG, et al. Experimental methodologies for the obtainment of *Momordica charantia* L. extracts with anthelmintic activity: a review. *Pharmaco Rev*. 2022;16(32):82–89.
11. Kumar DS, Xavier TF. Antibacterial activity, biosynthesis and characterization of silver nanoparticle from the leaf extract of (*L.*) *Nees. andrographis echinoides*. *Asian J Pharm Pharmacol*. 2019;5(1):95–100. <https://doi.org/10.31024/ajpp.2019.5.1.14>
12. Begum NA, Mondal S, Basu S, Laskar RA, Mandal D. Biogenic synthesis of Au and Ag nanoparticles using aqueous solutions of Black Tea leaf extracts. *Colloids Surf B*. 2009;71(1):113–118. <https://doi.org/10.1016/j.colsurfb.2009.01.012>

13. Kadam PV, Yadav KN, Deoda RS, Shivatare RS, Patil MJ. *Mimusops elengi*: a review on ethnobotany, phytochemical and pharmacological profile. *J Pharmaco Phytochem*. 2012;1(3):64–74.
14. Zahid H, Rizwani GH, Shareef H, Mahmud S, Ali T. Hypoglycemic and hypolipidemic effects of *Mimusops elengi* Linn, extracts on normoglycaemic and alloxaninduced diabetic rats. *Int J Pharmal Biol Arch*. 2012;3(1):56–62.
15. Gami B, Pathak S, Parabia M. Ethnobotanical, phytochemical and pharmacological review of *Mimusops elengi* Linn. *Asian Pa J Trop Biomed*. 2012;2(9):743–748. [https://doi.org/10.1016/S2221-1691\(12\)60221-4](https://doi.org/10.1016/S2221-1691(12)60221-4)
16. Nagajyothi P, Sreekanth T, Tetley CO, Jun YI, Mook SH. Characterization, antibacterial, antioxidant, and cytotoxic activities of ZnO nanoparticles using *Coptidis Rhizoma*. *Bioorg Med Chem Lett*. 2014;24(17):4298–4303. <https://doi.org/10.1016/j.bmcl.2014.07.023>
17. Gurgur E, Oluyamo S, Adetuyi A, Omotunde O, Okoronkwo A. Green synthesis of zinc oxide nanoparticles and zinc oxide–silver, zinc oxide–copper nanocomposites using *Bridelia ferruginea* as biotemplate. *SN Appl Sci*. 2020;2:1–12. <https://doi.org/10.1007/s42452-020-2269-3>
18. Talam S, Karumuri SR, Gunnam N. Synthesis, characterization, and spectroscopic properties of ZnO nanoparticles. *Int Scholar Res Not*. 2012;2012:e372505. <https://doi.org/10.5402/2012/372505>
19. Vijayalakshmi U, Chellappa M, Anjaneyulu U, Manivasagam G, Sethu S. Influence of coating parameter and sintering atmosphere on the corrosion resistance behavior of electrophoretically deposited composite coatings. *Mat Manufac Proc*. 2016;31(1):95–106. <https://doi.org/10.1080/10426914.2015.1070424>
20. Stan M, Popa A, Toloman D, Silipas T-D, Vodnar DC. Antibacterial and antioxidant activities of ZnO nanoparticles synthesized using extracts of *Allium sativum*, *Rosmarinus officinalis* and *Ocimum basilicum*. *Acta Metallur Sinica*. 2016;29:228–236. <https://doi.org/10.1007/s40195-016-0380-7>
21. Huang J, Li Q, Sun D, et al. Biosynthesis of silver and gold nanoparticles by novel sundried *Cinnamomum camphora* leaf.

- Nanotechnology*. 2007;18(10):e105104. <https://doi.org/10.1088/0957-4484/18/10/105104>
22. Shamhari NM, Wee BS, Chin SF, Kok KY. Synthesis and characterization of zinc oxide nanoparticles with small particle size distribution. *Acta Chim Sloven*. 2018;65(3):578–585. <https://doi.org/10.17344/acsi.2018.4213>
 23. Jayarambabu N, Kumari BS, Rao KV, Prabhu Y. Beneficial role of zinc oxide nanoparticles on green crop production. *Int J Multidiscip Adv Res Trends*. 2015;2:273–282.
 24. Jain N, Bhargava A, Majumdar S, Tarafdar J, Panwar J. Extracellular biosynthesis and characterization of silver nanoparticles using *Aspergillus flavus* NJP08: a mechanism perspective. *Nanoscale*. 2011;3(2):635–641. <https://doi.org/10.1039/C0NR00656D>
 25. Barzinjy AA, Azeez HH. Green synthesis and characterization of zinc oxide nanoparticles using *Eucalyptus globulus* Labill. leaf extract and zinc nitrate hexahydrate salt. *SN Appl Scis*. 2020;2(5):e991. <https://doi.org/10.1007/s42452-020-2813-1>
 26. Muhammad W, Ullah N, Haroon M, Abbasi BH. Optical, morphological and biological analysis of zinc oxide nanoparticles (ZnO NPs) using *Papaver somniferum* L. *RSC Adv*. 2019;9(51):29541–29548. <https://doi.org/10.1039/C9RA04424H>
 27. Khatami M, Alijani HQ, Heli H, Sharifi I. Rectangular shaped zinc oxide nanoparticles: green synthesis by *Stevia* and its biomedical efficiency. *Ceram Int*. 2018;44(13):15596–15602. <https://doi.org/10.1016/j.ceramint.2018.05.224>
 28. Khan MA, Abbasi BH, Shinwari ZK. Thidiazuron enhanced regeneration and silymarin content in *Silybum marianum* L. *Pak J Bot*. 2014;46(1):185–190.
 29. Ramesh M, Anbuvarannan M, Viruthagiri G. Green synthesis of ZnO nanoparticles using *Solanum nigrum* leaf extract and their antibacterial activity. *Spectrochim Acta A Mol Biomol Spectrosc*. 2015;136:864–870. <https://doi.org/10.1016/j.saa.2014.09.105>

30. Kumar SS, Venkateswarlu P, Rao VR, Rao GN. Synthesis, characterization and optical properties of zinc oxide nanoparticles. *Int Nano Lett.* 2013;3:e30. <https://doi.org/10.1186/2228-5326-3-30>
31. Fakhari S, Jamzad M, Fard HK. Green synthesis of zinc oxide nanoparticles: a comparison. *Green Chem Lett Rev.* 2019;12(1):19–24. <https://doi.org/10.1080/17518253.2018.1547925>
32. Raghupathi KR, Koodali RT, Manna AC. Size-dependent bacterial growth inhibition and mechanism of antibacterial activity of zinc oxide nanoparticles. *Langmuir.* 2011;27(7):4020–4028. <https://doi.org/10.1021/la104825u>
33. Ratney YJJ, David SB. Antibacterial activity of zinc oxide nanoparticles by sonochemical method and green method using *Zingiber officinale*. *Green Chem Tech Lett.* 2016;2:11–15. <https://doi.org/10.18510/gctl.2016.212>

Scientific Inquiry and Review (SIR)

Volume 7 Issue 4, 2023

ISSN (P): 2521-2427, ISSN (E): 2521-2435

Homepage: <https://journals.umt.edu.pk/index.php/SIR>



Article QR



Title: Development and Validation of RP-HPLC Method for Quantitative Analysis of Sulfamethoxazole and Trimethoprim in Liquid Suspension: A Comparative Study with Compendial Method

Author (s): Muhammad Aslam, Shahzad Ali, Mahmood Ahmed, Muhammad Aneeq Javed, Afsah Iftikhar, Yousaf Abbas, Aamir Sohail, Mehvish Abdul-Rehman, and Khansa Habibullah

Affiliation (s): University of Education, Lahore, Pakistan

DOI: <https://doi.org/10.32350/sir.74.02>

History: Received: April 16, 2023, Revised: September 7, 2023, Accepted: September 10, 2023, Published: 27 October, 2023

Citation: Aslam M, Ali S, Ahmed M, et al. Development and validation of RP-HPLC method for quantitative analysis of sulfamethoxazole and trimethoprim in liquid suspension: a comparative study with compendial method. *Sci Inq Rev.* 2023;7(4):19–34. <https://doi.org/10.32350/sir.74.02>

Copyright: © The Authors

Licensing:  This article is open access and is distributed under the terms of [Creative Commons Attribution 4.0 International License](https://creativecommons.org/licenses/by/4.0/)

Conflict of Interest: Author(s) declared no conflict of interest



A publication of
The School of Science
University of Management and Technology, Lahore, Pakistan

Development and Validation of RP-HPLC Method for Quantitative Analysis of Sulfamethoxazole and Trimethoprim in Liquid Suspension: A Comparative Study with Compendial Method

Muhammad Aslam*, Shahzad Ali, Mahmood Ahmed, Muhammad Aneeq Javed, Afsah Iftikhar, Yousaf Abbas, Aamir Sohail, Mehvish Abdul-Rehman, and Khansa Habibullah

Department of Chemistry, Division of Science and Technology, University of Education, Lahore, Pakistan

ABSTRACT

Co-trimoxazole is a combination of trimethoprim or sulfamethoxazole. It is used to treat common infectious diseases, including the lung disorders, urinary disorders, and gastrointestinal infections. The current study was performed to develop a new RP-HPLC technique. The main purpose was to analyze SMX (Sulfamethoxazole) and TMP (Trimethoprim) in a liquid medium of 60mL. The analyses of SMX and TMP were performed on RP-HPLC with a C18 column (25 cm × 4.6 mm) packed with 5 µm ODS, L1 stationary phase, while the mobile phase consisted of methanol and water with a ratio of 6:4. The pH of the system was adjusted to 2.6 by using dilute phosphoric acid. The injection volume was 20µL having a flow rate of 1 mL/minute and column temperature of 40°C. The analysis of all chromatograms was performed at a single wavelength of 254 nm. The validation of the method was determined for range, precision, linearity, specificity, accuracy, and system suitability. This method was found to be more environmentally friendly with respect to the other compendial methods, which are used for the TMP and SMX analysis.

Keywords: co-trimoxazole, chromatogram, RP-HPLC, sulfamethoxazole, trimethoprim

1. INTRODUCTION

Sulfamethoxazole (SMX) is an antibiotic drug that belongs to sulfanilamides [1]. It is utilized to address a range of health conditions that are generated within the body [2, 3]. These antibiotics can be provided to the body either through the mouth or by penetration through the injection [4]. They are quickly absorbed by the body and eliminated through the kidneys [5]. It is 4-amino-*N*-(5-methyl-1,2-oxazol-3-yl)benzene-1-

* Corresponding Author: maslamchemist@hotmail.com

sulfonamide. It is insoluble in water but easily soluble in acetone and sparingly soluble in alcohol [5, 6]. Trimethoprim (TMP) is a known biological agent, which inhibits bacterial activity. It is used to treat bacterial infections of the respiratory and urinary systems [7]. It is 2,4-diamino-5-(3'4'5'-trimethoxy benzyl)pyrimidine. These are white and cream colour substances [8]. The antibiotic mechanism of TMP is enhanced by sulfonamides [9]. They are used to cure bacterial infections [10]. The phenomenon of supra-additive takes place by sulfonamides addition. This is also the most common addition of multiple combinations for two antibiotic medicines of sulphamides. They have synergic effects and there is a 5:1 ratio of trimethoprim and sulfamethoxazole, respectively [11]. Their combination is known as co-trimoxazole, which is mainly used to treat lung disorders like pneumonia, Coccidiosis, diarrhea, and gastroenteritis. They are also used for hyper-alimentation in the form of an aqueous solution. Their injections can cure bacterial infections in cattle and horses [12, 13].

Previous research has described that there are many analytical tools to determine SMX and TMP; either in individual form or in combination form [14]. A number of HPLC (high-pressure liquid chromatography) methods have been used for the estimation of TMP and SMX in pharmaceutical or biological samples [15]. Reverse phase high-pressure liquid chromatography (RP-HPLC) is the most used HPLC having 65-90%, respectively [16]. Reasonably, its extensive use is because of its features, which are unity and ease of its use for handling those substances, which have very diverse polarity [17, 18]. Compendial methods are also used to know the quality level of various medicinal products. These methods are not validated [18, 19].

In this research study, the RP-HPLC method was developed and its validity was checked for the identification of SMX and TMP as compared to the compendial methods.

2. MATERIALS AND METHODS

2.1. Reagent and Chemicals

Trimethoprim and sulfamethoxazole were bought from Shandong Rongyuan Pharmaceutical Company Limited, China and Andhra Organics Limited, India, respectively. The distilled water of 0.01 $\mu\text{S}/\text{cm}$ conductivity was prepared in a laboratory. The source of methanol and orthophosphoric acid was Merck, Germany.

2.2. Instrumentation

The analyses were done by using the instruments including, Sonicator (Korea 60°C), aluminum foil (China 0.2 mm), hot plate (China 400°C), analytical balance (Sartorius, Germany Min 0.0001g: Max 320 g), column (Merck Germany, C₁₈), nylon filters (Sartorius, Germany 0.45µ), USA pH 0-14, pH metre (Jenco), vacuum pump (Japan 20psi), pH meter (Jenco 6173), Shimadzu LC-20AT Series with a dual pump, Dynamica, HALO DB-20 UV/Visible spectrophotometer, and 254 nm wavelength was used for analysis.

2.3. Collection of Samples

The standard molecules of SMX and TMP were taken from Andhra Organics Ltd. in India and Shandong Rongyuan Pharmaceutical Co., Ltd. in China with high purity levels of 99.44% and 99.66%, respectively, on an anhydrous basis.

2.4. Mobile Phase Preparation

The mobile phase was prepared by adding 600 mL of methanol in 400 mL of distilled water and adjusting the volume to the desired amount. The pH level of the solution was maintained at 2.6 level by adding a small amount of dilute phosphoric acid.

2.5. Standard Preparation

200 mg of sulfamethoxazole and 40 mg of trimethoprim were put into a flask of 100 mL. The mixture was diluted using methanol. A separate 50 mL volumetric flask was used to transfer 10 mL of this solution for further analysis.

2.6. Sample Preparation

To prepare the samples, 200 mg of SMX and 40 mg of TMP were added to a flask of 100 mL. From this solution, 10 mL was transferred to a 50 mL flask and the resulting solution was filtered. The concentration of TMP in the filtered solution was found to be 0.08 mg/mL and the concentration of SMX was found to be 0.4 mg/L.

2.7. Chromatographic System Configuration

The column used for analysis was 25 cm in length and 4.6 mm in diameter, it was also loaded with an ODS (octadecylsilyl) stationary phase

with a particle size of 5 μm , specifically the L1 type. The detector used in the analysis had a wavelength of 254 nm. The column was maintained at a temperature of 40°C and the flow rate of the mobile phase was set at 1 mL/minute. A sample injection volume of 20 μL was used for the analysis.

2.8. Method Validation

The developed method was validated through the following characteristics:

2.9. Linearity

Linearity is a measure of the relationship between the concentration of an analyte and the corresponding response of a measurement method. The coefficient of determination (r^2) of the regression line is used to determine the linearity of the method. For quantitative analysis, a value of r^2 greater than 0.99 generally denotes a strong linear connection between the analyte concentration and the observed response, which is considered acceptable. This indicates that the test results obtained by the technique will fall within a predictable range that is directly proportional to the analyte concentration that is being measured.

2.10. Specificity

The ability to dissociate analyte components in the presence of other components like matrix components is known as specificity [17]. If the method remained unaffected in the presence of impurities and exponents, it means that the method has specificity.

2.11. Accuracy

Accuracy is a measure of how closely an analytical method can determine the true value of a sample. An accurate method gave us an accurate value under different measurements. The accuracy of the method was shown because no divergence occurred from the true value. Accuracy reflects the degree to which an analytical method provides reliable and correct results that are free from significant errors or biases.

2.12. Precision

If the procedure is repeated multiple times for the samplings of a homogeneous sample and the results give closed values to each other, the analytical method is said to have precision.

3. RESULTS AND DISCUSSION

It is mandatory to analyze the drugs before their utilization. Analyzing data can provide both qualitative and quantitative information, which is crucially significant. Understanding the therapeutic mechanism of drugs is a vital aspect that cannot be overlooked. A number of methods are being used for simultaneous analysis of trimethoprim and sulfamethoxazole. FT-IR, amperometry, HPTLC, UV spectroscopy, and spectrometry were used for SMX and TMP analysis (see Table 1).

Table 1. Assay Calculations

Trimethoprim		Sulfamethoxazole	
Peak area of STD	Peak area of Sample	Peak area of STD	Peak area of sample
70503891	7729721	28393293	28691409
6940642	7688064	28513675	29049886
Average = 7708893		Average = 28870648	
Average	6997267	Average	28453484
S.D	80079.14	S.D	85122.93
RSD	1.144	RSD	0.299
Calculations of peak area of STD and sample			
Trimethoprim	7708893	37	100
	6997267	100	25
	101.57%		
Sulfamethoxazole	28870648	200.4	100
	28453484	100	25
	101.47%		

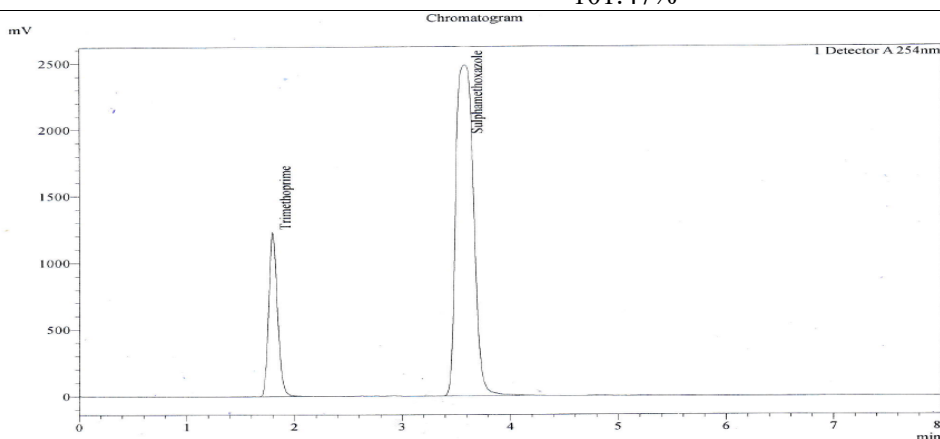


Figure 1. Chromatogram of TMP-SMZ Standard 1

Pharmaceutical industries specifically use RP-HPLC for conducting their analysis. The results obtained from the analysis of SMX and TMP are as follows (Figures 1 to 4; Tables 1-5).

Table 2. TMP-SMZ Standard 1 at 254 nm

Peak	Name	Area	Concentration	Tailing factor	Height	No. of theoretical plate
1	TMP	6940642	1.000	1.188	1229461	1969
2	SMZ	28393293	1.000	1.136	2483206	2819
Total		35333936			3712667	

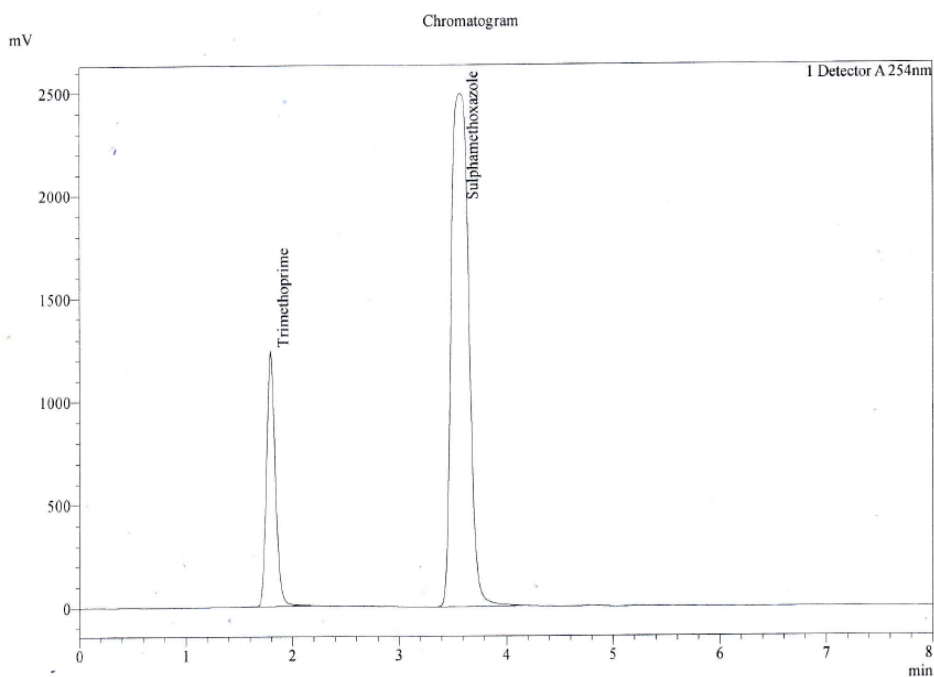


Figure 2. Chromatogram of TMP-SMZ Standard 2

Table 3. TMP-SMZ Standard 2 at 254 nm

Peak	Name	Tailing factor	Area	Height	Concentration	Number of theoretical plate
1	TMP	1.198	7053891	1233870	1.008	1948
2	SMZ	1.138	28513675	2488856	1.002	2797
Total			35567567	3722726		

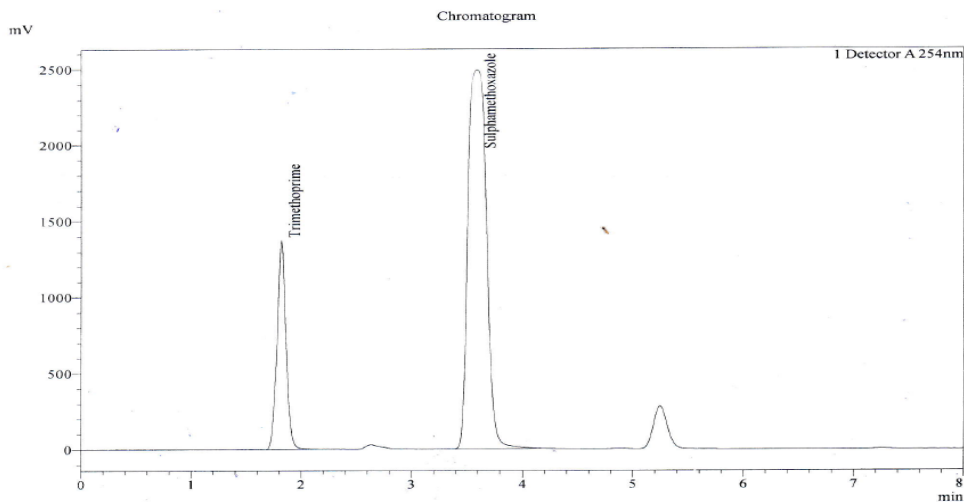


Figure 3. Chromatogram of TMP-SMZ Test Sample 1

Table 4. TMP-SMZ Test Sample 1 at 254 nm

Peak #	Name	Height	Area	Number of theoretical plate	Concentration	Tailing factor
1	TMP	1372780	7688064	2038	1.099	1.075
2	SMZ	2489631	2904986	2747	1.021	1.141
Total		3862411	3673790			

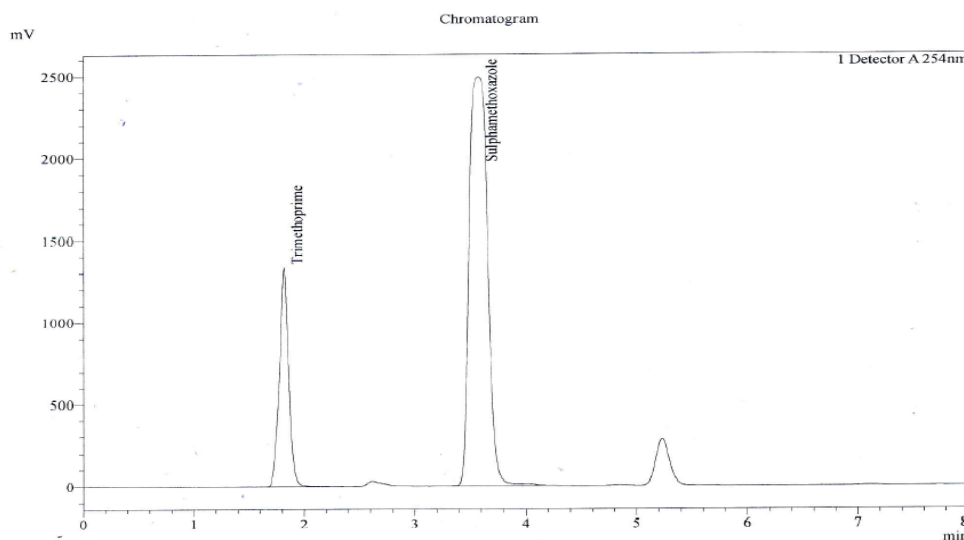


Figure 4. Chromatogram of TMP-SMZ Test Sample 2

Table 5. Results of TMP-SMZ Test Sample 2 at 254 nm

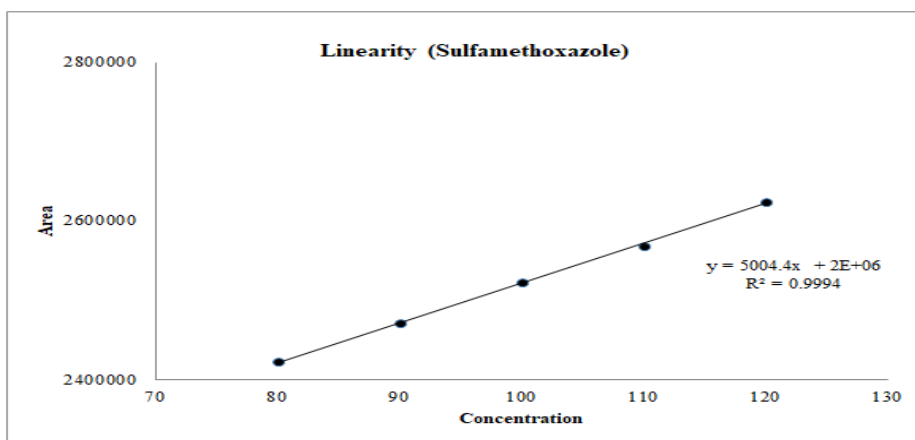
Peak	Name	Concentration	Area	Number of theoretical plate	Height	Tailing factor
1	TMP	1.105	7729721	1867	1333312	1.010
2	SMZ	1.008	28691409	2763	2488096	1.128
Total			36421130		3821408	

3.1. Method validation

3.1.1. Linearity. The method will show linearity if the results of the test are directly proportional to the quantity of the drug [18]. The percent concentrations of 80, 90, 100, 110, and 120 were injected, giving the following linearity results. Table 6 and Figure 5 & 6 show the results for the linearity.

Table 6. Linearity Values

Sr.#	Sample absorbance area		Solution volume (mL)	Conc. (mcg/mL)	% of drug
	Trimethoprim	Sulfamethoxazole			
1	2422329	16193821	25.6	4.0	80
2	2471764	16524307	28.8	4.5	90
3	2522209	16861538	32.0	5.0	100
4	2568653	17198768	35.2	5.5	110
5	2624106	17512744	38.4	6.0	120

**Figure 5.** Linearity (Sulfamethoxazole)

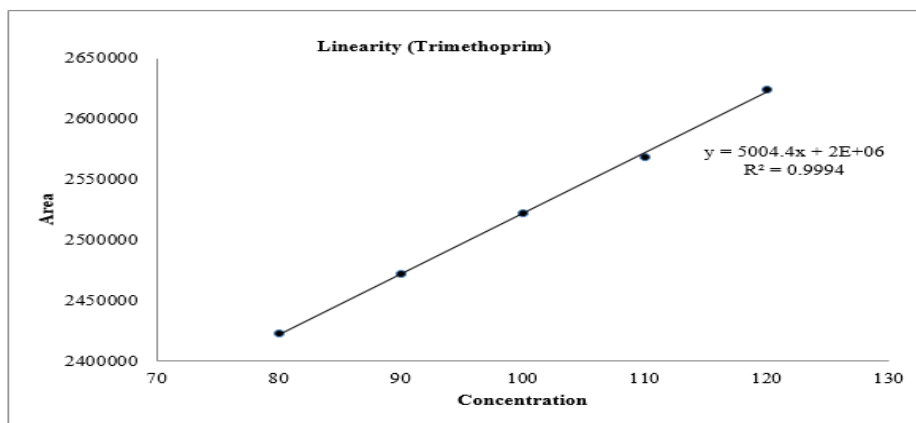


Figure 6. Linearity (Trimethoprim)

3.1.2. Specificity. Specificity is the ability of a solution in which components of the matrix dissolve the analyte. In the case of standard and placebo, the following results were obtained (see Table 7).

Table 7. Specificity

Sample	Standard samples (TMP/ SMX)	Placebo
Chromatogram (Peak Area / Spectrum)	Positive	Negative

3.1.3. Accuracy. Various trials were carried out to confirm the accuracy of this newly developed approach and the results are presented in Tables 8 and 9.

3.1.4. Sulfamethoxazole Results. Absorbance area of 80% reference: 16184214

Absorbance area of 100% reference: 16853525

Absorbance area of 120% reference: 17532744

Table 8. Accuracy Results for Sulfamethoxazole Samples

In placebo percentage of active	120%		100%		80%	
Absorbance area of test solution	17524535	17545738	16870344	16880168	16205637	16190974

Label claim (%)	99.95%	100.04%	100.10%	100.16%	100.13%	100.07%
Deviation from calculated results	0.05%	0.07%	0.10%	0.16%	0.13%	0.04%
Average recovery	100.01%		100.13%		100.08%	

Table 9. Accuracy Results for Trimethoprim Samples

TMP Content added in placebo	120%		100%		80%	
Absorbance area of test solution	2624684	2628955	2524891	2528142	2419311	2421047
Label claim (%)	99.98%	100.14%	100.07%	100.20%	99.96%	100.03%
Deviation from calculated results	0.02%	0.14%	0.07%	0.20%	0.04%	0.03%
Average Recovery	100.06%		100.13%		99.99%	

3.1.5. Precision. If there is a degree of closeness between the individual test findings, the procedure has precision. The following results were obtained for instrument precision (see Table 10).

Table 10. Instrument precision

Sr. No.	Area of Internal Standard (Sulfamethoxazole)	Areas of standards (Trimethoprim)
1.	16852548	2499147
2.	16850018	2498046
3.	16861538	2522209
4.	16841827	2546895
5.	16791588	2506789
RSD	0.1645%	0.8137%
S.D	27692.63	20461.58
Mean	16839503.8	2514617.2

3.2. Method Precision

It was expressed as RSD and found out by:

3.2.1. Repeatability. The assay was performed on separate samples in 3 replicate sets (see Tables 11 and 12).

3.2.1.1. Sulfamethoxazole Results. Absorbance area of the reference: 16835314

Concentration of reference: 32 µg/ml

Wavelength: 254 nm

3.2.1.2. Trimethoprim Results. Absorbance area of the reference: 2519356

Concentration of reference: 32 µg/ml

Wavelength: 254 nm

Table 11. Repeatability of Sulfamethoxazole Samples

Repeatability (Sulfamethoxazole)					
Samples		Absorbance Area	Analyte concentration (µg/ml)	%results	Deviation from calculated results
I	1	16794517	32	99.76	0.24%
	2	16840138	32	100.03	0.03%
	3	16841974	32	100.04	0.04%
II	4	16863183	32	100.17	0.17%
	5	16874201	32	100.23	0.23%
	6	16806357	32	99.83	0.17%

SD = 0.1849; Average = 100.01%; RSD = 0.1849%

Table 12. Repeatability of Trimethoprim Samples

		Repeatability (Trimethoprim)			
Samples		Analyte concentration (µg/ml)	% results	Area of absorbance	Deviation from calculated results
II	1	32	100.04	2520302	0.04%
	2	32	99.96	2518346	0.04%
	3	32	100.44	2530556	0.44%

Repeatability (Trimethoprim)					
Samples		Analyte concentration (µg/ml)	% results	Area of absorbance	Deviation from calculated results
II I	4	32	100.41	2529654	0.41%
	5	32	99.91	2517178	0.09%
	6	32	100.2	02524356	0.20%

Average = 100.16%; SD = 0.2280; RSD = 0.2277%

3.2.2. Reproducibility. The term reproducibility describes how effectively an analytical process may be used by many analysts working in the same laboratory. The following results were obtained when the assay was performed on three distinct samples as indicated in (see Tables 13 and 14).

3.2.2.1. Sulfamethoxazole Results. Absorbance area of the reference: 16813456

Concentration of reference: 32 µg/ml

Wavelength: 254 nm

3.2.2.2. Trimethoprim Results. Absorbance area of the reference: 2516209

Concentration of reference: 32 µg/ml

Wavelength: 254 nm

Table 13. Reproducibility of Sulfamethoxazole Samples

Samples	Reproducibility			
	Analyte concentration (µg/ml)	% results	Absorbance area	Variation from theoretical results (%)
1	32	99.97	16808945	0.03
2	32	100.12	16832952	0.12
3	32	100.10	16829435	0.10

SD = 0.0771; RSD = 0.0770%; Mean = 100.06%

Table 14. Reproducibility of Trimethoprim Samples

Samples	Reproducibility			
	Analyte concentration (µg/ml)	% results	Absorbance area	Fluctuation from theoretical results (%)
1	32	100.49	2528516	0.49
2	32	100.11	2519063	0.11
3	32	100.23	2521964	0.23

Mean = 100.28%; SD = 0.1924; RSD = 0.1919%

The RP-HPLC method developed in this research study was found to be the most effective method among all, which covers all the analytical techniques [15–17]. It was also observed that this technique was better than compendial methods since it is free of pollution, which showed that it is environmentally friendly. The mobile phase is methanol: water (6:4). The pH of the mobile phase was maintained at 2.6 level by using dilute phosphoric acid. The combined determination of Sulfamethoxazole and Trimethoprim requires this pollution-free analysis.

4. CONCLUSION

The current study concluded that the newly developed RP-HPLC method was cost-effective and convenient to use. It also fulfilled all the validation parameters like linearity, specificity, accuracy, and precision. The primary significance of this method lies in its environmentally friendly nature and suitability for our environment. Further studies can be used for the determination of impurities in samples using the LC-MS technique and future researchers can further establish their research by using this study results.

REFERENCES

1. Akay C, Özkan SA. Simultaneous LC determination of trimethoprim and sulphamethoxazole in pharmaceutical formulations. *J Pharm Biomed Anal.* 2002;30(4):1207–1213. [https://doi.org/10.1016/s0731-7085\(02\)00460-0](https://doi.org/10.1016/s0731-7085(02)00460-0)
2. Al-Saidi KH, Yonis MS. Simultaneous determination of sulphamethoxazole and trimethoprim in binary mixtures and in tablet using derivative spectrophotometry. *J Al-Nahrain Uni.* 2018;18(1):46–54.

3. Cribb AE, Spielberg SP. Sulfamethoxazole is metabolized to the hydroxylamine in humans. *Clin Pharm Therap.* 1992;51(5):522–526. <https://doi.org/10.1038/clpt.1992.57>
4. Dantas RF, Contreras S, Sans C, Esplugas S. Sulfamethoxazole abatement by means of ozonation. *J Hazard Mater.* 2008;150(3):790–794. <https://doi.org/10.1016/j.jhazmat.2007.05.034>
5. Roedel MM, Nakada SY, Penniston KL. Sulfamethoxazole-induced sulfamethoxazole urolithiasis: a case report. *BMC Urol.* 2021;21(133):1–5. <https://doi.org/10.1186/s12894-021-00894-5>
6. Shewiyo DH, Kaale E, Risha PG, Dejaegher B, Smeyers-Verbeke J, Vander-Heyden, Y. Development and validation of a normal-phase high-performance thin layer chromatographic method for the analysis of sulfamethoxazole and trimethoprim in co-trimoxazole tablets. *J Chromatogr A.* 2009;1216(42):7102–7107. <https://doi.org/10.1016/j.chroma.2009.08.076>
7. Abass AM, Alabdullah S, Salman, HG. Determination of trimethoprim by various analytical techniques- A – review. *Int J Res Eng Inno.* 2020;4(1):1–4. <http://doi.org/10.36037/IJREI.2020.4101>
8. Gonzalez D, Melloni C, Poindexter BB, et al. Simultaneous determination of trimethoprim and sulfamethoxazole in dried plasma and urine spots. *Bioanalysis.* 2015;7(9):1137–1149. <https://doi.org/10.4155/bio.15.38>
9. Rajith L, Kumar KG. Electroanalysis of trimethoprim on metalloporphyrin incorporated glassy carbon electrode. *Drug Test Anal.* 2010;2(9):436–441. <https://doi.org/10.1002/dta.161>
10. Bushby SRM, Hitchings GH. Trimethoprim, a sulphonamide potentiator. *Br J Pharmacol Chemothera.* 1968;33(1):72–90. <https://doi.org/10.1111/j.1476-5381.1968.tb00475.x>
11. Gurumurthy T, Monika M, Ashwini V. Development and validation RP-HPLC method for simultaneous estimation of Sulfamethoxazole and Trimethoprim. *Ind J Biotech Pharm Res.* 2017;5(3):235–238.
12. Abraham SA, Abass AM, Ahmed A. Trimethoprim determination with drug-selective electrodes. *Asian J Pharm Clin Res.* 2019;12(6):83–87.

13. Darrell JH, Garrod LP, Waterworth PM. Trimethoprim: laboratory and clinical studies. *J Clin Pathol.* 1968;21(2):202–209. <https://doi.org/10.1136/jcp.21.2.202>
14. Yao J, Shi YQ, Li ZR, Jin SH. Development of a RP-HPLC method for screening potentially counterfeit anti-diabetic drugs. *J Chromatogr B.* 2007;853(1-2):254–259. <https://doi.org/10.1016/j.jchromb.2007.03.022>
15. Kaila HO, Ambasana MA, Thakkar RS, Saravaia HT, Shah AK. A new improved RP-HPLC method for assay of rosuvastatin calcium in tablets *Ind J Pharm Sci.* 2010;72(5):592–598. <https://doi.org/10.4103/0250-474X.78526>
16. Yabré M, Ferey L, Somé IT, Gaudin K. Greening reversed-phase liquid chromatography methods using alternative solvents for pharmaceutical analysis. *Molecules.* 2018;23(5):1–25. <https://doi.org/10.3390/molecules23051065>
17. Braun AC, Ilko D, Merget B, et al. Predicting critical micelle concentration and micelle molecular weight of polysorbate 80 using compendial methods. *Eur J Pharm Biopharm.* 2015;94:559–568. <https://doi.org/10.1016/j.ejpb.2014.12.015>
18. Speer I, Preis M, Breitzkreutz J. Dissolution testing of oral film preparations: Experimental comparison of compendial and non-compendial methods. *Int J Pharm.* 2019;561:124–134. <https://doi.org/10.1016/j.ijpharm.2019.02.042>
19. Van den Bossche L, Lodi A, Schaar J, et al. An interlaboratory study on the suitability of a gradient LC-UV method as a compendial method for the determination of erythromycin and its related substances. *J Pharm Biomed Anal.* 2010;53(1):109–112. <https://doi.org/10.1016/j.jpba.2010.03.012>

Scientific Inquiry and Review (SIR)

Volume 7 Issue 4, 2023

ISSN (P): 2521-2427, ISSN (E): 2521-2435

Homepage: <https://journals.umt.edu.pk/index.php/SIR>



Article QR



Title: Coefficient Inequalities for Certain Subclass of Starlike Function with respect to Symmetric points related to q-exponential Function

Author (s): Zameer Abbas, Sadia Riaz


Affiliation (s): Department of Mathematics, National University of Modern Languages, Islamabad, Pakistan

DOI: <https://doi.org/10.32350/sir.74.03>

History: Received: May 7, 2023, Revised: October 7, 2023, Accepted: October 7, 2023, Published: October 27, 2023.

Citation: Abbas Z, Riaz S. Coefficient inequalities for certain subclass of starlike function with respect to symmetric points related to q-exponential function. *Sci Inq Rev.* 2023;7(4):35–52. <https://doi.org/10.32350/sir.74.03>

Copyright: © The Authors

Licensing:  This article is open access and is distributed under the terms of [Creative Commons Attribution 4.0 International License](https://creativecommons.org/licenses/by/4.0/)

Conflict of Interest: Author(s) declared no conflict of interest



UMT

A publication of
The School of Science
University of Management and Technology, Lahore, Pakistan

Coefficient Inequalities for Certain Subclass of Starlike Function with respect to Symmetric points related to q -exponential Function

Zameer Abbas^{*}, and Sadia Riaz

Department of Mathematics, National University of Modern Languages,
Islamabad, Pakistan

ABSTRACT

The current study aims to define a class of starlike functions with respect to symmetric points subordinated with q -exponential functions. Furthermore, to investigate the coefficient inequalities and possible upper-bound of the third-order Hankel determinant for the functions belonging to our new class this study observed the new and already derived results for further analysis.

Keywords: analytic function, Hankel Determinant, q -derivative, symmetric point

1. INTRODUCTION

The analytic functions, also called holomorphic functions, are complex-valued functions that are defined and differentiable at every point within their domain of definition. The class of all analytical functions f with the normalized condition in the open unit disc $E = \{z: |z| < 1\}$ is asymbol by A and has the Taylor series, which is stated as:

$$f(z) = z + a_2z^2 + a_3z^3 + a_4z^4 + \dots \quad (1.1)$$

The class of univalent and analytical function unit disc E is proved by S. Caratheodory functions are a class of complex-valued functions, which are defined on a domain in the complex plane. They are named after the mathematician Constant in Caratheodory symbolized by and the function of this class is of the form

$$p(z) = 1 + p_1z + p_2z^2 + p_3z^3 + p_4z^4 + \dots \quad (1.2)$$

The Schwarz function, named after the German mathematician Hermann Schwarz, is a complex-valued function that maps the unit disk E in the complex planes to itself. It is known by $f(z) = \frac{-z}{1-z^2}$ where z is a complex number. Specifically, if f and g are analytic functions defined on some domain D , then $f < g$ if there lie other analytic functions h defined

^{*} Corresponding Author: zameermaths01@gmail.com

on D such as $f(z) = g(h(z)) \forall z$ in D . Thomas [1], and Pommerenke [2] defined the Hankel determinant $H_k(c)$, for positive integer k, c for the function in S . In the form eq (1), as shown below:

$$H_k(c) = \begin{vmatrix} a_n & a_{n+1} & \cdots & a_{n+q-1} \\ a_{n+1} & a_{n+2} & \cdots & a_{n+q} \\ \vdots & \vdots & \ddots & \vdots \\ a_{n+q-1} & a_{n+q} & \cdots & a_{n+2q-2} \end{vmatrix} \quad (1.3)$$

For fixedly positive integers k and c the growths of $H_k(c)$ as $n \rightarrow \infty$ have been determined by Obradovic [3], In 2023, with a boundedness boundary. Ehrenborg [4] investigated the Hankel determinant for exponential polynomials. The Hankel determinant of differentiable orders is achieved for k, c differential rates. For instance, when $k = 2$ and $c = 1$ it is defined as,

$$H_2(1) = \begin{vmatrix} a_1 & a_2 \\ a_2 & a_3 \end{vmatrix}, |a_1 a_3 - a_2^2| a_1 = 1 \quad (1.4)$$

The Fekete-Szego inequality is a well-known result in complex analysis and potential theory that provides an estimate for the growth of the Taylor coefficients of function that are analytical unit disk E . More precisely, let $f(z)$ be functions that are analytical in the open unit disc $|z| < 1$, and let its Taylor series expansions be given by (1). In 2023, Singh et al. [5] and Fekete-Szego defined an inequality for the coefficient of a univalent analytic function on the unit disk. The Fekete-Szego inequality for some normalized analytic functions was investigated by various researchers working in the field of Geometric Functions Theory like Choi et al. [6], Ali et al. [7, 8], Owa and Cho [9, 10], Orhan and Cotirla [11], and Murugusundaramoorthy et al. [12]. In 2006, Shanmugam et al. [13] introduced The Fekete-Szego problem that can be applied to sub-classes of star-like functions when considering symmetrical points. Now for $k = 2, c = 2$ it can be obtained as,

$$H_2(2) = \begin{vmatrix} a_2 & a_3 \\ a_3 & a_4 \end{vmatrix}, |a_2 a_4 - a_3^2| \quad (1.5)$$

In 2012, Krishna and Ramreddy [14] introduced the 2nd Hankel determinant of means the univalent function, which is discussed here. Using a indeed close p , valent function the growth rate of the 2nd Hankel determinant was calculated by Shrigan [15] in 2022. Other researchers like Janteng et al. [16, 17], Bansal [18], Lee et al. [19], Lei et al. [20], Rain et al. [21], Rajya et al. [22], Zaprawa [23] introduced the coefficient of the function f that belong to the sub-class S of univalent function or to its sub-classes the upper-bound of the Hankel determinant for $k = 2, c = 3$ such as, $H_2(3)$ is defined as:

$$H_2(3) = \begin{vmatrix} a_3 & a_4 \\ a_4 & a_5 \end{vmatrix}, \quad |a_3 a_5 - a_4^2| \quad (1.6)$$

For $k = 3, c = 1$ the Hankel Determinant, $H_3(1)$ is known as the 3rd Hankel Determinant we have

$$H_3(1) = \begin{vmatrix} a_1 & a_2 & a_3 \\ a_2 & a_3 & a_4 \\ a_3 & a_4 & a_5 \end{vmatrix} \quad (1.7)$$

$$a_3(a_2 a_4 - a_3^2) - a_4(a_1 a_4 - a_2 a_3) + a_5(a_3 - a_2^2), \quad a_1 = 1$$

1.1. Applications

In mathematical physics, analytic functions are crucial for solving two-dimensional issues. Displacements and stresses in antiplane or in-plane fracture problems can be expressed as functions of complex potentials. Hankel matrices are created when an underlying state-space model or hidden Markov model is desired as a given sequence of output data. The A, B, and C matrices that characterize the state-space realization can be computed using the singular value decomposition of the Hankel matrix. The breakdown of non-stationary signals and time-frequency representation has been proven to be advantageous when using the Hankel matrix created from the signal. To get the weight parameters for the polynomial distribution approximation, the method of moments applied to polynomial distributions produces a Hankel matrix that must be inverted [24].

Calculus uses course equivalent q -calculus which is based on the solution of logical q -analogous outcomes without the use of limits. The systematic introduction of q -calculus is credited to Lashin [25]. Khanetal

[26] introduced and presented definitions for q -derivative. q -derivative of functions f be a normalized-analytic function is known as

$$D_q f(z) = \frac{f(qz) - f(z)}{(q-1)z}, z \neq 0,$$

and $D_q f(0) = f'(0)$ where $q \in (0, 1)$ taking $q \rightarrow 1^-$ we get $D_q f \rightarrow f'$.

In 2007, Babalola [27] was defined as the 1st person to analyze the upper-bound of the 3rd Hankel determinant for sub-classes of S^* . Other researchers like Vamshee Krishna et al. [28], Patil and Khairnar [29], Prajapat et al. [30], Yalcin and Altinkaya [31], Cho et al. [32], Lecko et al. [33], Kowalczyk et al. [34], Mohd Narzan et al. [35], Several other researchers like Mendiratta et al. [36], Haiyan Zhang et al. [37], Khan et al. [38], and Senguttuvan et al. [39] defined a thorough sub-class of analytic functions with respect to the symmetrical point that has been developed. The current study is expanded by using quantum calculus and tends to investigate the upper bounds of the 3rd Hankel Determinant, for the classes of a star-like function with respect to symmetrical points subordinate to exponential functions. Mahmood et al. [40] Shi et al. [41], Verma et al. [42], Viswanadh et al. [43], Omer [44], Joshi et al. [45], Breaz et al [46], Wang [47], and investigated the class of univalent function star-like with respect to symmetrical points. Here, the following subclass of starlike function are defined below:

Definition 1.1. A function $f \in A$ and f is known to be in the class $S_s^*(e^{qz})$ as

$$\frac{2[zf'(z)]}{f(z)-f(-z)} \prec e^{qz}, z \in E, \quad (1.8)$$

we note that taking $q \rightarrow 1^-$ in the above definition, we obtain the known class $S_s^*(e^z)$ see [48]. The following Lemmas are required to demonstrate the intended outcomes.

Lemma 1.1. [49] If $p \in P$, then $|p_n| \leq 2, \forall n \in N$.

Lemma 1.2. [50] If $p(z) = 1 + p_1z + p_2z^2 + p_3z^3 + \dots$ is such that $Re(p(z)) > 0$ in E , then for some x, z with $|x| \leq 1, |z| \leq 1$, we have

$$2p_2 = p_1^2 + x(4 - p_1^2), \text{ for some } x, |x| \leq 1 \quad (1.9)$$

$$4p_3 = p_1^3 + 2p_1(4 - p_1^2)x - p_1(4 - p_1^2)x^2 + 2(4 - p_1^2)(1 - |x|^2)z \quad (1.10)$$

Lemma 1.3. [51] If $p \in P$, then $|p_2 - vp_1^2| \leq \max \{|1, |2v - 1|\}$ for any $v \in \mathbb{C}$.

3. MAIN RESULTS

Theorem.3.1: If $f \in S_s^*(e^{qz})$ then $|a_2| \leq \frac{q}{2}$, $|a_3| \leq \frac{q}{2}$, $|a_4| \leq \left| \frac{q}{4} + \left(\frac{-4q+3q^2}{8} \right) + \left(\frac{12q-18q^2+5q^3}{48} \right) \right|$, $|a_5| \leq \left| \frac{q}{4} + \left(\frac{-2q+q^2}{4} \right) + \left(\frac{-6q+9q^2-3q^3+q^4}{24} \right) \right|$.

Proof: As $f \in S_s^*(e^{qz})$ as

$$\frac{2[zf'(z)]}{f(z) - f(-z)} = e^{qw(z)}. \quad (2.1)$$

Using **Eq. (2.1)**, we consider

$$\frac{2[zf'(z)]}{f(z) - f(-z)} = 1 + 2a_2z + 2a_3z^2 + (4a_4z^4 - 2a_3a_2)z^3 + (4a_5z^5 - 2a_3^2)z^4 + \dots \quad (2.2)$$

Let us define the function,

$$p(z) = \frac{1 + qw(z)}{1 - qw(z)}.$$

Equivalent,

$$qw(z) = \frac{p(z)-1}{p(z)+1}, \quad (2.3)$$

Consider

$$qw(z) = \frac{p_1z}{2} + \left(\frac{p_2}{2} - \frac{p_1^2}{4} \right) z^2 + \left(\frac{p_3}{2} - \frac{p_1p_2}{2} + \frac{p_1^3}{8} \right) z^3 + \left(\frac{p_4}{2} - \frac{p_1p_4}{2} - \frac{p_2^2}{4} + \frac{3p_1^2p_2}{8} - \frac{p_1^4}{16} \right) z^4 \dots \quad (2.4)$$

Since we have

$$e^{qw(z)} = 1 + qw(z) + \frac{(qw(z))^2}{2!} + \frac{(qw(z))^3}{3!} + \frac{(qw(z))^4}{4!} + \dots \quad (2.5)$$

We get

$$e^{qw(z)} = 1 + \frac{qp_1z}{2} + \left(\frac{p_2}{2} - \frac{p_1^2}{8}\right)q + \left(\frac{p_1^2q^2}{8}\right)z^2 + \left(\frac{p_3}{2} - \frac{p_1p_2}{4} + \frac{p_1^3}{48}\right)q +$$

$$\left(\frac{-p_1^2q^2}{8} + \frac{p_1p_2q^2}{4} + \frac{p_1^3q^3}{48}\right)z^3 + \left(\frac{p_4}{2} - \frac{p_1p_3}{4} - \frac{p_2^2}{8} + \frac{p_1^2p_2}{16} + \frac{p_1^4}{384}\right)q +$$

$$\left(\frac{p_2^2}{8} + \frac{3p_1^4}{32} - \frac{p_1^2p_2}{4} + \frac{p_1p_3}{4}\right)q^2 + \left(-\frac{p_1^2p_2}{16} - \frac{p_1^4}{32}\right)q^3 + \left(\frac{p_1^4q^4}{384}\right)z^4 + \dots \quad (2.6)$$

From **Eq. (2.2)** and **Eq. (2.6)**, we compare the coefficient, and we get

$$a_2 \leq \frac{qp_1}{4}, a_3 = \left(\frac{p_2}{4} - \frac{p_1^2}{8}\right)q + \frac{q^2p_1^2}{16},$$

$$a_4 = \frac{p_3q}{8} - \frac{p_1p_2q}{8} + \frac{3p_1p_2q^2}{32} + \frac{p_1^3q}{32} - \frac{p_1^3q^2}{64} + \frac{5p_1^3q^3}{384},$$

$$a_5 = \left(\frac{p_4q}{8} + \left(-\frac{p_1p_3q}{8} + \frac{p_1p_3q^2}{16}\right) + \left(\frac{3p_1^2p_2q}{32} - \frac{3p_1^2p_2}{32} - \frac{3p_1^2p_2q^2}{32}\right) + \right.$$

$$\left.\left(\frac{p_1^4q^2}{128} - \frac{p_1^4q}{64} - \frac{p_1^4q^3}{128} + \frac{p_1^4q^4}{384}\right)\right). \quad (2.7)$$

By using **Lemma 1.1** and **Lemma 1.3** in **Eq. (2.7)**, we get

$$|a_2| \leq \frac{q}{2}, |a_3| \leq \frac{q}{2}, |a_4| \leq \left|\frac{q}{4} + \left(\frac{-4q + 3q^2}{8}\right) + \left(\frac{12q - 18q^2 + 5q^3}{48}\right)\right|,$$

$$|a_5| \leq \left|\frac{q}{4} + \left(\frac{-2q + q^2}{4}\right) + \left(\frac{-6q + 9q^2 - 3q^3 + q^4}{24}\right)\right|. \quad (2.8)$$

which are the required results.

Theorem 3.2: If $f \in S_s^*(e^{qz})$ then $|a_3 - a_2^2| \leq \frac{q}{2}$

Proof: From **Eq. (2.7)** in **Theorem 3.1** we have

$$a_2 \leq \frac{qp_1}{4}, a_3 = \left(\frac{p_2}{4} - \frac{p_1^2}{8}\right)q + \frac{q^2p_1^2}{16}. \quad (2.9)$$

On simplifying, we get

$$|a_3 - a_2^2| = \left|\frac{qp_2}{4} - \frac{q^2p_1^2}{8}\right|. \quad (2.10)$$

By using **Lemma 1.3**, we get

$$|a_3 - a_2^2| \leq \frac{q}{2}. \quad (2.11)$$

which are the required results.

Theorem 3.3: If $f \in S_s^*(e^{qz})$ then $|a_2a_3 - a_4| \leq$

$$\begin{aligned} & \frac{1}{48(q^2-6q-12)} \left(3q \left(3q \left(-\frac{2(-4+\sqrt{-2q^3+8q^2+48q+64})}{q^2-6q-12} \right) q^4 - \right. \right. \\ & 36q \left(-\frac{2(-4+\sqrt{-2q^3+8q^2+48q+64})}{q^2-6q-12} \right)^2 q^3 + \\ & 6q \left(-\frac{2(-4+\sqrt{-2q^3+8q^2+48q+64})}{q^2-6q-12} \right) q^4 + 12q^5 + \\ & 2q^4 \sqrt{-2q^3+8q^2+48q+64} + 36q \left(-\frac{2(-4+\sqrt{-2q^3+8q^2+48q+64})}{q^2-6q-12} \right)^2 q^2 - \\ & 72q \left(-\frac{2(-4+\sqrt{-2q^3+8q^2+48q+64})}{q^2-6q-12} \right) q^3 - 144q^4 - \\ & 8\sqrt{-2q^3+8q^2+48q+64} q^3 + 432q \left(-\frac{2(-4+\sqrt{-2q^3+8q^2+48q+64})}{q^2-6q-12} \right)^2 q + \\ & 72q \left(-\frac{2(-4+\sqrt{-2q^3+8q^2+48q+64})}{q^2-6q-12} \right) q^2 + 144q^3 - \\ & 48\sqrt{-2q^3+8q^2+48q+64} q^2 + 432q \left(-\frac{2(-4+\sqrt{-2q^3+8q^2+48q+64})}{q^2-6q-12} \right)^2 + \\ & 864q \left(-\frac{2(-4+\sqrt{-2q^3+8q^2+48q+64})}{q^2-6q-12} \right) q + 1728q^2 - \\ & 16\sqrt{-2q^3+8q^2+48q+64} q + 864q \left(-\frac{2(-4+\sqrt{-2q^3+8q^2+48q+64})}{q^2-6q-12} \right) + \\ & 1600q. \end{aligned}$$

Proof: From Eq. (2.7) of Theorem 3.1, we have

$$|a_2a_3 - a_4| = \left| \frac{q^2p_1p_2}{16} - \frac{p_1^3q^2}{32} + \frac{q^3p_1^3}{64} - \frac{p_3q}{8} + \frac{p_1p_2q}{8} - \frac{3p_1p_2q^2}{32} - \frac{p_1^3q^2}{32} + \frac{p_1^3q^2}{64} - \frac{5p_1^3q^3}{384} \right|. \quad (2.12)$$

Denotes $|x| = t \in [0,1]$, $p_1 = e \in [0,2]$, using triangle inequality (2.12) we have

$$|a_2a_3 - a_4| \leq \frac{e(4-e^2)qt^2}{32} - \frac{t(4-e^2)q^2e}{64} - \frac{q(4-e^2)}{16} + \frac{e^3q^3}{384},$$

suppose that

$$F(e, 1) \equiv \frac{e(4-e^2)qt^2}{32} - \frac{t(4-e^2)q^2e}{64} - \frac{q(4-e^2)}{16} + \frac{e^3q^3}{384}.$$

Thus, we get $\frac{\partial F}{\partial t} = \frac{(4-e^2)etq}{16} - \frac{(4-e^2)eq^2}{64} \geq 0$, the function $F(e,t)$ is non-decreasing for any t in $[0,1]$. this show that $F(e,t)$ has max value at $t=1$.

$$\text{Max}F(e, t) = F(e, 1) = \frac{e(4-e^2)qt^2}{32} - \frac{t(4-e^2)q^2e}{64} - \frac{q(4-e^2)}{16} + \frac{e^3q^3}{384},$$

which implies that

$$M(e) = \frac{e(4-e^2)qt^2}{32} - \frac{t(4-e^2)q^2e}{64} - \frac{q(4-e^2)}{16} + \frac{e^3q^3}{384},$$

Then,

$$M'(e) = \left(-\frac{qe^2}{16} + \frac{(-e^2+4)q}{32} - \frac{e^2q^2}{32} - \frac{(-e^2+4)q^2}{64} - \frac{eq}{8} + \frac{e^2q^3}{128} \right),$$

$$M'(e) = \text{be lost } e = m^* = -\frac{2(-4+\sqrt{-2q^3+8q^2+48q+64})}{q^2-6q-12}.$$

A simple computational yield that $M''(e) < 0$, which means that the functions $M(e)$ can take a max value at $m^* = -\frac{2(-4+\sqrt{-2q^3+8q^2+48q+64})}{q^2-6q-12}$.

Hence we get

$$\begin{aligned} |a_2a_3 - a_4| &\leq \frac{1}{48(q^2-6q-12)} \left(3q \left(3q \left(-\frac{2(-4+\sqrt{-2q^3+8q^2+48q+64})}{q^2-6q-12} \right) q^4 - \right. \right. \\ &36q \left(-\frac{2(-4+\sqrt{-2q^3+8q^2+48q+64})}{q^2-6q-12} \right)^2 q^3 + \\ &6q \left(-\frac{2(-4+\sqrt{-2q^3+8q^2+48q+64})}{q^2-6q-12} \right) q^4 + 12q^5 + \\ &2q^4 \sqrt{-2q^3+8q^2+48q+64} + 36q \left(-\frac{2(-4+\sqrt{-2q^3+8q^2+48q+64})}{q^2-6q-12} \right)^2 q^2 - \\ &72q \left(-\frac{2(-4+\sqrt{-2q^3+8q^2+48q+64})}{q^2-6q-12} \right) q^3 - 144q^4 - \\ &8\sqrt{-2q^3+8q^2+48q+64} q^3 + 432q \left(-\frac{2(-4+\sqrt{-2q^3+8q^2+48q+64})}{q^2-6q-12} \right)^2 q + \\ &72q \left(-\frac{2(-4+\sqrt{-2q^3+8q^2+48q+64})}{q^2-6q-12} \right) q^2 + 144q^3 - \\ &48\sqrt{-2q^3+8q^2+48q+64} q^2 + 432q \left(-\frac{2(-4+\sqrt{-2q^3+8q^2+48q+64})}{q^2-6q-12} \right)^2 + \\ &864q \left(-\frac{2(-4+\sqrt{-2q^3+8q^2+48q+64})}{q^2-6q-12} \right) q + 1728q^2 - \end{aligned}$$

$$16\sqrt{-2q^3 + 8q^2 + 48q + 64}q + 864q \left(-\frac{2(-4 + \sqrt{-2q^3 + 8q^2 + 48q + 64})}{q^2 - 6q - 12} \right) + 1600q. \quad (2.13)$$

which are the required results.

Theorem 3.4: If $f \in S_s^*(e^{qz})$ then $|a_2a_4 - a_3^2| \leq \frac{3q^2}{8}$

Proof: From Eq. (2.7) of Theorem 3.4, we have

$$|a_2a_4 - a_3^2| = \left| \frac{p_1p_3q^2}{32} + \frac{3p_1^2p_3q^3}{128} - \frac{p_1^2p_3q^2}{32} + \frac{p_1^4q^2}{128} - \frac{3p_1^4q^3}{256} + \frac{5p_1^4q^4}{1536} - \frac{p_1^2p_2}{128} - \frac{p_1^4}{1536} - \frac{p_2^2q^2}{16} - \frac{p_2p_1^2q^3}{32} + \frac{p_2p_1^2q^2}{16} \right|,$$

we use the Lemma 1.3 we have

$$|a_2a_4 - a_3^2| = \left| \frac{p_1q^2(4-p_1^2)(1-|x|^2)z}{64} - \frac{p_1^2(4-p_1^2)x^2q^2}{128} + \frac{3p_1^2q^3x(4-p_1^2)}{256} - \frac{x^2q^2(4-p_1^2)^2}{64} + \frac{5p_1^4q^4}{1536} - \frac{p_1^4q^2}{64} + \frac{p_1^4q^2}{32} - \frac{p_1^4q^4}{64} - \frac{p_1^4q^4}{256} \right|. \quad (2.14)$$

Denotes $|x| = t \in [0,1]$, $p_1 = e \in [0,2]$ then using tri-angle inequality we have

$$|a_2a_4 - a_3^2| \leq \frac{q^2(4-e^2)}{32} + \frac{e^2(4-e^2)t^2q^2}{128} + \frac{3e^2q^3t(4-e^2)}{256} + \frac{t^2q^2(4-e^2)^2}{64} + \left(\frac{5e^4q^4}{1536} - \frac{e^4q^2}{64} + \frac{e^4q^2}{32} - \frac{e^4q^4}{64} - \frac{e^4q^4}{256} \right), \quad (2.15)$$

which implies that

$$F(e, t) = \frac{q^2(4-e^2)}{32} + \frac{e^2(4-e^2)t^2q^2}{128} + \frac{3e^2q^3t(4-e^2)}{256} + \frac{t^2q^2(4-e^2)^2}{64} + \left(\frac{5e^4q^4}{1536} - \frac{e^4q^2}{64} + \frac{e^4q^2}{32} - \frac{e^4q^4}{64} - \frac{e^4q^4}{256} \right). \quad (2.16)$$

Thus, we get

$$\frac{\partial F}{\partial t} = \frac{3(4-e^2)e^2q^2}{256} + \frac{(4-e^2)e^2q^2}{64} + \frac{(4-e^2)^2q^2t}{32} + \frac{(4-e^2)e^2q^2t}{64} \geq 0,$$

which gives that $F(e, t)$ is increasing for any then t in $[0,1]$, this show that $F(e, t)$ has a maxi value at $t = 1$.

$$\begin{aligned} \text{Max } F(e, t) = F(e, t) &= \frac{q^2(4-e^2)}{32} + \frac{e^2(4-e^2)t^2q^2}{128} + \frac{3e^2q^3t(4-e^2)}{256} + \\ &+ \frac{t^2q^2(4-e^2)^2}{64} + \left(\frac{5e^4q^4}{1536} - \frac{e^4q^2}{64} + \frac{e^4q^2}{32} - \frac{e^4q^4}{64} - \frac{e^4q^4}{256} \right). \end{aligned} \quad (2.17)$$

Let us define

$$\begin{aligned} M(c) &= \frac{q^2(4-e^2)}{32} + \frac{e^2(4-e^2)t^2q^2}{128} + \frac{3e^2q^3t(4-e^2)}{256} + \frac{t^2q^2(4-e^2)^2}{64} + \left(\frac{5e^4q^4}{1536} - \right. \\ &\left. \frac{e^4q^2}{64} + \frac{e^4q^2}{32} - \frac{e^4q^4}{64} - \frac{e^4q^4}{256} \right). \end{aligned} \quad (2.18)$$

We have

$$M'(e) = \frac{5e^3q^2}{128} - \frac{(-5e^2 + 4)eq^2}{128} - \frac{(eq^2)e}{16} - \frac{25e^3q^4}{384},$$

$M'(e)$ vanishes at $e = 0$. A simple compilation yield that $M''(e) < 0$, which mean that the functions $M(e)$ has max values at $e = 0$. We get

$$|a_2a_4 - a_3^2| \leq M(0) = \frac{3q^2}{8}, \quad (2.19)$$

which are the required results.

Theorem 3.5: If $f \in S_s^*(e^{qz})$ then $|H_3(1) =$

$$\begin{aligned} &\frac{1}{2304(q^2-6q-12)^2} \left(q^3 \left(-\frac{2(-4+\sqrt{-2q^3+8q^2+48q+64})}{q^2-6q-12} \right)^2 q^4 - \right. \\ &180q \left(-\frac{2(-4+\sqrt{-2q^3+8q^2+48q+64})}{q^2-6q-12} \right)^2 q^3 + \\ &30q \left(-\frac{2(-4+\sqrt{-2q^3+8q^2+48q+64})}{q^2-6q-12} \right) q^4 + \\ &10q^4 \sqrt{-2q^3+8q^2+48q+64} + 60q^5 + \\ &180q \left(-\frac{2(-4+\sqrt{-2q^3+8q^2+48q+64})}{q^2-6q-12} \right)^2 q^2 - \\ &360q \left(-\frac{2(-4+\sqrt{-2q^3+8q^2+48q+64})}{q^2-6q-12} \right) q^4 - \\ &40\sqrt{-2q^3+8q^2+48q+64}q^3 - 288q^4 + \\ &\left. 2160q \left(-\frac{2(-4+\sqrt{-2q^3+8q^2+48q+64})}{q^2-6q-12} \right)^2 q + \right) \end{aligned}$$

$$\begin{aligned}
& 360q \left(-\frac{2(-4+\sqrt{-2q^3+8q^2+48q+64})}{q^2-6q-12} \right) q^2 - \\
& 240\sqrt{-2q^3+8q^2+48q+64} q^2 - 4464q^3 + \\
& 2160q \left(-\frac{2(-4+\sqrt{-2q^3+8q^2+48q+64})}{q^2-6q-12} \right)^2 + \\
& 4320q \left(-\frac{2(-4+\sqrt{-2q^3+8q^2+48q+64})}{q^2-6q-12} \right) q - \\
& 80\sqrt{-2q^3+8q^2+48q+64} q + 13824q^2 + \\
& 4320q \left(-\frac{2(-4+\sqrt{-2q^3+8q^2+48q+64})}{q^2-6q-12} \right) + 702008q + 62208 \Big) + \\
& \frac{1}{2} \left(\frac{1}{4}q - \frac{1}{8}q^2 - \frac{1}{8}q^3 + \frac{1}{24}q^4 \right) q.
\end{aligned}$$

Proof: $H_3(1) = a_3(a_2a_4 - a_2^2) - a_4(a_1a_4 - a_2a_3) + a_5(a_3 - a_2^2), a_1 = 1$

(2.20)

By applying triangle inequality, we get

Now, substituting the Eq. (2.8),(2.11),(2.13),(2.19), in (2.20) we get

$$\begin{aligned}
|H_3(1)| & \leq \frac{1}{2304(q^2-6q-12)^2} \left(q^3 \left(15q \left(-\frac{2(-4+\sqrt{-2q^3+8q^2+48q+64})}{q^2-6q-12} \right)^2 q^4 - \right. \right. \\
& 180q \left(-\frac{2(-4+\sqrt{-2q^3+8q^2+48q+64})}{q^2-6q-12} \right)^2 q^3 + \\
& 30q \left(-\frac{2(-4+\sqrt{-2q^3+8q^2+48q+64})}{q^2-6q-12} \right) q^4 + \\
& 10q^4\sqrt{-2q^3+8q^2+48q+64} + 60q^5 + \\
& 180q \left(-\frac{2(-4+\sqrt{-2q^3+8q^2+48q+64})}{q^2-6q-12} \right)^2 q^2 - \\
& 360q \left(-\frac{2(-4+\sqrt{-2q^3+8q^2+48q+64})}{q^2-6q-12} \right) q^4 - \\
& 40\sqrt{-2q^3+8q^2+48q+64} q^3 - 288q^4 + \\
& \left. 2160q \left(-\frac{2(-4+\sqrt{-2q^3+8q^2+48q+64})}{q^2-6q-12} \right)^2 q + \right)
\end{aligned}$$

$$\begin{aligned}
 & 360q \left(-\frac{2(-4+\sqrt{-2q^3+8q^2+48q+64})}{q^2-6q-12} \right) q^2 - \\
 & 240\sqrt{-2q^3+8q^2+48q+64} q^2 - 4464q^3 + \\
 & 2160q \left(-\frac{2(-4+\sqrt{-2q^3+8q^2+48q+64})}{q^2-6q-12} \right)^2 + \\
 & 4320q \left(-\frac{2(-4+\sqrt{-2q^3+8q^2+48q+64})}{q^2-6q-12} \right) q - \\
 & 80\sqrt{-2q^3+8q^2+48q+64} q + 13824q^2 + \\
 & 4320q \left(-\frac{2(-4+\sqrt{-2q^3+8q^2+48q+64})}{q^2-6q-12} \right) + 702008q + 62208 \Big) + \\
 & \frac{1}{2} \left(\frac{1}{4}q - \frac{1}{8}q^2 - \frac{1}{8}q^3 + \frac{1}{24}q^4 \right) q, \tag{2.21}
 \end{aligned}$$

which are the required results.

4. DISCUSSION

The coefficients of the univalent functions attracted the attention of researchers working in the field of Geometric Functions Theory. On the other hand, Quantum Calculus and Quantum theory have been applied to the concepts of Geometric Functions Theory to advance the known classes and results. The Fekete-Szegő problem are a well-known coefficient problem in this field which has a variety of application in other sciences. The well-known application of the Fekete problem is the Hankel determinant. The Hankel determinant of order two have been investigated by various researchers in this field but the 3rd order Hankel determinant for starlike functions with respect to symmetric points have attained the attention of researcher nowadays. To fill this research gap we have worked on the 3rd order Hankel determinant for our new class of starlike functions with respect to symmetric points subordination q -exponential function. Where the concepts of quantum calculus and q -derivative operator have been applied. The current study determined that on taking $q \rightarrow 1^-$ for the result proved in this research article, similar results were obtained that were already proved in [47].

4.1. Conclusion

The class of starlike functions with respect to symmetric points and the q -extension of these class has been investigated. Conclusively, a new class

of starlike functions with respect to symmetric points associated with q -exponential function by using the subordination technique is defined and studied in this research. Some remarkable results, including coefficient inequalities, the Fekete Szegő problem, and the third-order Hankel determinant have been investigated. It was indicated that the new class along with the associated main theorems are the advancement of the results and classes, which has already been studied by the researcher working in the field of Geometry Functions Theory (GFT).

REFERENCES

1. Thomas DK, Tuneski N, Vasudevarao A. *Univalent Functions a Primer*. vol. 69. Walter de Gruyter GmbH & Co KG; 2018.
2. Răducanu D, Zaprawa P. Second Hankel determinant for close-to-convex functions. *Comptes Rendus Math.* 2017;355(10):1063–1071. <http://doi:10.1016/j.crma.2017.09.006>
3. Obradović M, Tuneski N. Hankel determinants of second and third order for the class \mathcal{S} of univalent functions. *Math Slovaca.* 2021;71(3):649–654. <http://doi:10.1515/ms-2021-0010>
4. Ehrenborg R. The Hankel determinant of exponential polynomials. *Amer Math Monthly.* 2000;107(6):557–560. <http://doi:10.1080/00029890.2000.12005236>
5. Singh G, Singh G. Coefficient bounds for a generalized subclass of bounded turning functions associated with Sigmoid function (in press). *Int J Nonlinear Anal Appl.* 2023. <http://dx.doi.org/10.22075/ijnaa.2023.29574.4195>
6. Choi JH, Kim YC, Sugawa T. A general approach to the Fekete-Szegő problem. *J Math Soc Japan.* 2007;59(3):707–727. <http://doi:10.2969/jmsj/05930707>
7. Lee SK, Ali RM, Ravichandran V, Supramaniam S. The Fekete-Szegő coefficient functional for transforms of analytic functions. *Bulletin Iran Math Soc.* 2011;35(2):119–142.
8. Ali RM, Ravichandran V, Seenivasagan N. Coefficient bounds for p -valent functions. *Appl Math Comput.* 2007;187(1):35–46. <http://doi:10.1016/j.amc.2006.08.100>
9. Cho NE, Owa S. On the Fekete-Szegő problem for strongly-quasi convex functions. *Amkang J Math.* 2003;34(1):21–28.
10. Cho NE, Owa S. On the Fekete-Szegő problem for strongly-logarithmic quasi-convex functions. *Southeast Asian Bull Math.* 2004;28(3):1–11.

11. Orhan H, Cotîrlă LI. Fekete-Szegő inequalities for some certain subclass of analytic functions defined with ruscheweyh derivative operator. *Axioms*. 2022;11(10):e560. <http://doi:10.3390/axioms11100560>
12. Murugusundaramoorthy G, Kavitha S, Rosy T. On the Fekete Szegő problem for some subclasses of analytic functions defined by convolution. *Proc Pakistan Acad Sci*. 2007;44(4):249–254.
13. Shanmugam TN, Ramachandran C, Ravichandran V. Fekete-Szegő problem for subclasses of starlike functions with respect to symmetric points. *Bull Korean Math Soc*. 2006;43(3):589–598.
14. Krishna DV, Ramreddy T. Coefficient inequality for certain subclasses of analytic functions. *New Zealand J Math*. 2012;42:217–228.
15. Shrigan MG. An upper bound to the second Hankel determinant for a new class of univalent functions. *Asian-Euro J Math*. 2022;16(5):e2350092. <http://doi:10.1142/S1793557123500924>
16. Janteng A, Halim SA, Maslina D. Coefficient inequality for a function whose derivative has a positive real part. *J Inequal Pure Appl Math*. 2006;7(2):1–5.
17. Janteng A, Halim SA, Maslina D. Hankel determinant for starlike and convex functions. *Int J Math Anal*. 2007;1(13-16):619–625.
18. Bansal D. Upper bound of second Hankel determinant for a new class of analytic functions. *Appl Math Lett*. 2013;26(1):103–107. <http://doi:10.1016/j.aml.2012.04.002>
19. Lee SK, Ravichandran V, Supramaniam S. Bounds for the second Hankel determinant of certain univalent functions. *J Inequal Appl*. 2013;2013:e281. <http://doi:10.1186/1029-242X-2013-281>
20. Liu MS, Xu JF, Yang M. Upper bound of second Hankel determinant for certain subclasses of analytic functions. *Abstr Appl Anal*. 2014;2014:e603180. <http://doi:10.1155/2014/603180>
21. Raina RK, Sokol J. On coefficient estimates for a certain class of starlike functions. *Hacet J Math Stat*. 2015;44(6):1427–1433.
22. Laxmi KR, Sharma RB. Second Hankel determinants for some subclasses of biunivalent functions associated with pseudostarlike functions. *J Complex Anal*. 2017;2017:e6476391. <http://doi:10.1155/2017/6476391>
23. Zaprawa P. On Hankel determinant $H_2(3)$ for univalent functions. *Results Math*. 2018;73(3):e89. <http://doi:10.1007/s00025-018-0854-1>

24. Munkhammar J, Mattsson L, Rydén J. Polynomial probability distribution estimation using the method of moments. *PLOS ONE*. 2017;12(4):e0174573. <http://doi:10.1371/journal.pone.0174573>
25. Lashin AMY, Algethami BM, Badghaish AO. Convolution Properties of Certain Classes of Analytic Functions Defined by Jackson q -Derivative. *Mathematics*. 2021;10(1):e105. <http://doi:10.3390/math10010105>
26. Khan B, Srivastava HM, Tahir M, Darus M, Ahmad QZ, Khan N. Applications of a certain q -integral operator to the subclasses of analytic and bi-univalent functions. *AIMS Math*. 2021;6:1024–1039. <http://doi:10.3934/math.2021061>
27. Babalola KO. On Hankel determinant for some classes of univalent functions. *Inequal Theory Appl*. 2007;6:1–7.
28. Krishna DV, Venkateswarlu B, RamReddy T. Third Hankel determinant for starlike and convex functions concerning symmetric points. *Ann Univ Mariae Curie-Skłodowska Sect*. 2016;70(1):37–45.
29. Patil SM, Khairnar SM. Third Hankel determinant for starlike function with respect to symmetric points. *Int J Pure Appl Math Sci*. 2017;10(1):7–15.
30. Prajapat JK, Bansal D, Maharana S. Bounds on third Hankel determinant for certain classes of analytic functions. *Stud Univ Babes-Bolyai Math*. 2017;62(2):183–195. <http://doi:10.24193/subbmath.2017.2.05>
31. Altinkaya S, Yalcin S. Third Hankel determinant for Bazilevic functions. *Adv Math*. 2016;5(2):91–96.
32. Cho NE, Kowalczyk B, Kwon OS, Lecko A, Sim YJ. Some coefficient inequalities related to the Hankel determinant for strong starlike functions of order α . *J Math Inequal*. 2017;11(2):429–439.
33. Lecko A, Sim YJ, Smiarowska B. The sharp bound of the Hankel determinant of the third kind for starlike functions of order $1/2$. *Complex Anal Oper Theory*. 2018;12(4):819–827. <http://doi:10.1007/s11785-018-0819-0>
34. Kowalczyk B, Lecko A, Sim YJ. The sharp bound for the Hankel determinant of the third kind for convex functions. *Bull Aust Math Soc*. 2018;97(3):435–445.
35. Mohammed Pauzi MN, Darus M, Saibah Siregar. Second and third Hankel determinant for a class defined by generalized polylogarithm functions. *Transylvanian J Math Mech*. 2018;10(1):31–41.

36. Mendiratta R, Nagpal S, Ravichandran V. On a subclass of strongly starlike functions associated with exponential function. *Bull Malays Math Sci Soc.* 2015;38(1):365–386. <http://doi:10.1007/s40840-014-0026-8>
37. Zhang HY, Tang H, Niu XM. Third Order Hankel determinant for a certain class of analytic functions related with exponential function. *Symmetry.* 2018;10(10):e501. <http://doi:10.3390/sym10100501>
38. Khan MG, Ahmad B, Murugusundaramoorthy G, et al. Third Hankel determinant and Zalcman functional for a class of starlike functions with respect to symmetric points related with sine function. *J Math Comput Sci.* 2022;25:29–36.
39. Senguttuvan A, Mohankumar D, Ganapathy RR, Karthikeyan KR. Coefficient inequalities of a comprehensive subclass of analytic functions with respect to symmetric points. *Malaysian J Math Sci.* 2022;16(3):437–450. <http://doi:10.47836/mjms.16.3.03>
40. Mahmood S, Srivastava HM, Malik SN. Some subclasses of uniformly univalent functions with respect to symmetric points. *Symmetry.* 2019;11(2):e287. <http://doi:10.3390/sym11020287>
41. Shi L, Shutaywi M, Alreshidi N, Arif M, Ghufra SM. The sharp bounds of the third-order Hankel determinant for certain analytic functions associated with an eight-shaped domain. *Fractal Fractional.* 2022;6(4):e223. <http://doi:10.3390/fractalfract6040223>
42. Verma N, Kumar SS. On sharp third Hankel determinant for certain starlike functions. *arXiv.* 2022:earXiv:2211.14527. <http://doi:10.48550/arXiv.2211.14527>
43. Viswanadh GKS, Rath B, Kumar KS, Krishna DV. The sharp bound for the third hankel determinant of the inverse of functions associated with lemniscate of bernoulli. *Asian-Euro J Math.* 2023;16(07):e2350126. <http://doi:10.1142/S1793557123501267>
44. Omer SO, Aamir M, Bilal M, Ullah K, Qadir A. Study of second-order Hankel determinant for starlike functions with respect to symmetric points. *VFAST Transac Math.* 2023;11(1):52–66.
45. Joshi K, Kumar SS. Third Hankel determinant for a class of starlike functions associated with exponential function. *ArXiv.* 2022;earXiv:2206.13707. <http://doi:10.48550/arXiv.2206.13707>
46. Breaz D, Cătaș A, Cotîrlă LI. On the upper bound of the third Hankel determinant for certain class of analytic functions related with exponential function. *Analele științifice ale Universității "Ovidius"*

- Constanța. *Seria Matemat.* 2022;30(1):75–89. <http://doi:10.2478/auom-2022-0005>
47. Ganesh K, Sharma RB, Laxmi KR. Third Hankel determinant for a class of functions with respect to symmetric points associated with exponential function. *WSEAS Trans Math.* 2020;19:e13. <http://doi:10.37394/23206.2020.19.1>
48. Libera RJ, Zlotkiewicz EJ. Coefficient bounds for the inverse of a function with derivative in. *Proc Amer Math Soc.* 1983;87(2):251–257.
49. Wang ZG, Arif M, Liu ZH, et al. Sharp bounds of Hankel determinants for certain subclass of starlike functions. *J Appl Anal Comput.* 2023;13:860–873. <http://doi.org/10.11948/20220180>
50. Pommerenke Ch. Univalent functions. *J Math Soc Japan.* 1975;49:759–780.
51. Ravichandran V, Polatoglu Y, Bolcal M, Sen A. Certain subclasses of starlike and convex functions of complex order. *Hacet J Math Stat.* 2005;34:9–15.

Scientific Inquiry and Review (SIR)

Volume 7 Issue 4, 2023

ISSN (P): 2521-2427, ISSN (E): 2521-2435

Homepage: <https://journals.umt.edu.pk/index.php/SIR>



Article QR



Title: Properties of Graph Based on Divisor-Euler Functions

Author (s): Asif Abd ur Rehman, Muhammad Khalid Mahmood


Affiliation (s): University of the Punjab, Lahore, Pakistan

DOI: <https://doi.org/10.32350/sir.74.04>

History: Received: May 3, 2023, Revised: September 13, 2023, Accepted: September 15, 2023,
Published: October 30, 2023

Citation: Rehman AA, Mahmood MK. Properties of graph based on Divisor-Euler functions. *Sci Inq Rev.* 2023;7(4):53–66. <https://doi.org/10.32350/sir.74.04>

Copyright: © The Authors

Licensing:  This article is open access and is distributed under the terms of [Creative Commons Attribution 4.0 International License](https://creativecommons.org/licenses/by/4.0/)

Conflict of Interest: Author(s) declared no conflict of interest



UMT

A publication of
The School of Science
University of Management and Technology, Lahore, Pakistan

Properties of Graph Based on Divisor-Euler Functions

Asif Abd ur Rehman* and M. Khalid Mahmood

Department of Mathematics University of the Punjab, Lahore, Pakistan

ABSTRACT

Divisor function $D(n)$ gives the residues of n which divide it. A function denoted by $\tau(n)$ counts the total possible divisors of n and ϕ gives the list of co-prime integers to n . Many graphs had been constructed over these arithmetic functions. Using $D(n)$ and $\phi(n)$, a well known graph named as divisor Euler function graph has been constructed. In this paper, we use divisor function and anti Euler function ϕ' . We label the symbol $\phi^c(n)$ to count those residues of n which are not co-prime to n . By using these functions, we find a new graph, called divisor anti-Euler function graph (DAEFG), denoted as $G(d(\phi^c(n)))$. Let $G(d(\phi^c(n))) = (\mathbb{V}, \mathbb{E})$ be a DAEFG, where $\mathbb{V} = \{d_i \mid d_i \mid n\}$ and $\mathbb{E} = \{d_i d_j \mid \gcd(d_i, d_j) \neq 1\}$. The objective of this sequel is to introduce and discuss the properties of DAEFG. In this work, we discuss novel classes of proposed graph with its structure using loops, cycles, components of graph, degree of its vertices, components as complete, bipartite, planar, Hamiltonian and Eulerian graphs. Also, we find chromatic number, chromatic index and clique of these graphs.

Keywords: divisor function, divisor Euler function graph, divisor Euler function sub-graph, Euler function graph, metric dimension, resolvent.

1. INTRODUCTION

The systematic use of number theoretic functions in combinatorial mathematics is an interesting and useful task nowadays. Recently, the study of graphs based on number theoretic functions has become much more motivating. In our work, we use three number theoretic functions and define a new class of graph based on these functions. We familiarize and study the structures of such graphs. Such construction of graphs based on number theory leads to many new useful results. This area of mathematics has a wide range of applications in chemistry, computer science, navigation, robot science and engineering as well. The notion of divisor graph was first introduced by Singh and Santhosh in 2000. In 2015, K. Kannan et al. [1]

* Corresponding Author: asifrehman.math@gmail.com

presented a graph of number theoretic function namely, the divisor function graph. He suggested an idea for constructing graphs on divisors of integers by taking as vertices. We denote the set $D(n) = \{d_j: d_j \mid n, d_j \leq n\}$ as the set of positive divisors of n . In his contribution, both vertices and edges were based on $D(n)$. Shanmugavelan constructed a graph, namely Euler's phi function graph based on Euler's phi function [2]. He constructed this graph by taking a set of nodes and a set of edges based on this function $\phi(n)$. Using these co-prime residues, an idea of prime labeling has been introduced and investigated in [3]. Over n vertices, the formula for finding the maximal number of edges in this type of labeling has been established as $\Sigma\phi(n)$ in [3]. The well-known Cayley graph associated with the totient function, known as the Cayley totient graph [4], contains residues modulo s namely $\{0, 1, 2, \dots, n-1\}$ with the edge set $\{(a, b)/a-b \in T\}$. It is denoted by $\mathbb{G}(\phi(Z_n))$, where T denotes all positive integers which are less than n and co-prime to n . In the following paragraph, a few definitions are addressed to make this study self-contained.

Metric dimension is an attractive parameter in graph theory. The idea of resolving set for a connected graph was firstly first used by Slater [5] and [6], where he termed it as a locating set. He referred to the least locating set as a reference set and its cardinality as the Metric dimension, which has a wide range of applications in many fields of chemistry computer science physics and robot science. The distance between any two vertices is denoted as $d(u, v)$ which gives the minimum number of edges needed to transverse to reach from u to v . Let \mathbb{G} be a graph with one component i.e., a connected graph, a node t resolves a pair of vertices u and v of $\mathbb{V}(\mathbb{G})$ if $d(u, t) \neq d(v, t)$. If a subset $\mathfrak{R} \subseteq \mathbb{V}$ resolves the whole set of nodes, then \mathfrak{R} is called a resolving set (RS). General results on MD were discussed in [12]. Eccentricity of a particular vertex u is defined as the maximum distance between any of the vertices of the graph with v that is $\text{ecc}(v) = \max\{d(w, v); w \text{ lies in } \mathbb{V}(\mathbb{G})\}$. Many useful results regarding FMD and LFMD were discussed in [7] and [8], respectively. Results regarding algorithm and graph labeling were discussed in [9–11]. Many results on digraphs and their labeling based on number theory are discussed in [12–15]. Results on upper bound sequence of networks and RN's via Lambert type Map can be seen in [16–18]. Useful results on further graph theoretic applications are widely discussed in [19–21]. Research on degree and connection-based Zagreb indices of the network is astonishing nowadays.

Fruitful results of such newly defined degree based topological invariants of the M-polynomial, tadepol graph are discussed in [22] and [23]. Computation of entropy measures and valency-based indices of networks are discussed in [24] and [25]. The results of connection based such indices of networks are given in [26–28].

A loop (or a fixed point) in a graph is a vertex that is adjacent to itself, and it is called an isolated vertex if it is not adjacent to any other vertex. The vertices v_1, v_2, \dots, v_n will form a cycle of length n if v_1 is adjacent to v_2 , v_2 is adjacent to v_3 , and so on till v_n is adjacent to v_1 . A maximal connected subgraph is termed as a component. The number of vertices adjacent to a vertex v is called its degree. A graph is complete if all vertices are adjacent to the rest of all vertices. A graph is termed as bipartite if its set of vertices can be partitioned into two disjoint sets such that any two vertices in a set are not adjacent to each other. A graph is regular if all vertices have same degree. A graph is said to be planar if it can be drawn on a plane such that no two edges intersect each other except the end points. A graph is termed as Hamiltonian if it has a cycle through all vertices and visits each vertex exactly one time. While a graph is Eulerian if each of its vertex has an even degree. The chromatic number is the smallest number of colors that can be assigned to its vertices such that no two same colors are adjacent or no two adjacent vertices have same color and the minimum number of colors such that no two adjacent edges have same color. Lastly, the order of a maximal complete subgraph is called a clique of that graph. Now, we recall a few well-known definitions and results from number theory which will be used in the sequel to make this paper self-contained. The following definitions can be found in [7].

Definition 1.1. [4] Arithmetic functions are those functions, which are defined for all positive integers, such as Divisor function $d(n)$, Euler Phi function $\phi(n)$, Tau Function $\tau(n)$, Sigma function $\sigma(n)$ and Anti- Euler function ϕ' etc.

Definition 1.2. [4] Divisor function $d(n)$ is the set of those numbers which are less than or equal to n and which divides n . For example, for $n = 10$, $d(n) = \{1, 2, 5, 10\}$

Definition 1.3. [2] Divisor Euler function graph $G = (V, E)$ is a graph in which set of nodes are based on divisor function and set of edges is based

on Euler phi function and any two nodes are adjacent if these are co-prime to each other.

Definition 1.4. [2] Divisor-not prime function graph is a graph in which set of nodes is based on divisor function and any two nodes are adjacent if these are not prime to each other. It is also termed as divisor anti Euler function graph.

Definition 1.5. [4] Divisor Euler function graph denoted by $\phi(n)$ is a graph in which the number of integers from the set $\{1, 2, \dots, n-1\}$ are relatively prime to n , i.e., $\phi(n) = 1$.

Definition 1.6. [4] The number of integers from the set $\{1, 2, \dots, n-1\}$ which are not relatively prime to n is the function $\phi'(n)$. $\phi'(n)$ denotes the numbers that are less than or equal to n and non-prime to n . Since $\phi(n) = n-1$ for n be any prime but $\phi'(n) = 1$, for $n = 5, \phi'(n) = 1$, and $\phi'(8) = 4$, and these numbers are 2, 4, 6 and 8 as these are all non-prime to n , i.e., $(8, 20) \neq 1$

Theorem 1.1. [4] For any integer n , $\phi(n) = n-1$ if and only if n is prime. So, $\phi'(n) = 1$.

Theorem 1.2. [4] If n is any prime, then $\phi(n^k) = n^{k-1}(n-1)$, $k \geq 1$.

Theorem 1.3. [4] If m and n are any two co-prime integers, then $\phi(mn) = \phi(m)\phi(n)$.

Definition 1.7. Divisor anti Euler function graph (DAEFG) labeled as $G(d(\phi'(n)))$ with $V = \{d_i : d_i | n\}$ and $E = \{d_i d_j : \gcd(d_i, d_j) \neq 1, \forall d_i, d_j \in V\}$. The DAEFG for $n = 8$ and $n = 12$ are depicted in Fig. 1.

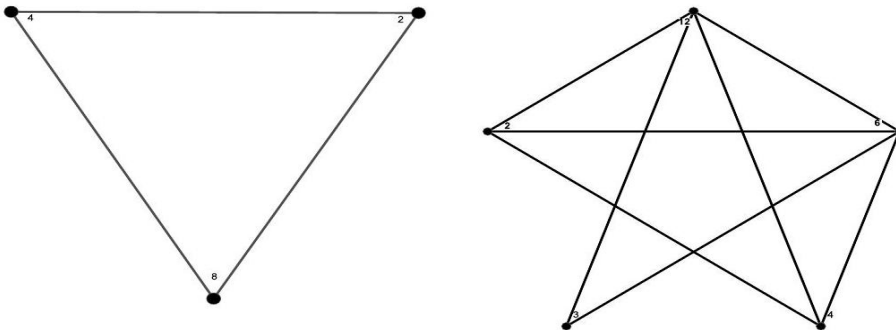


Figure 1. DAEFG for $n = 8$ and $n = 12$

2. STRUCTURES IN DAEFG

Corollary 2.1. $G(d(\phi'(n)))$ has exactly 2 components.

Corollary 2.2. $\deg(v(1)) = 0$.

Corollary 2.3. The largest of any vertex d in DAEFG is $\tau(n) - 2$.

Proof: The proof is simple. Since node 1 is isolated which clearly depicts that no other node can have an edge with node 1. So, there are total $\tau(n) - 1$ nodes in the connected part of graph. As by definition graph is simple so there is no loop. So, there are $\tau(n) - 2$ total number of possible edges incident with node n . Hence, it is the only node with the largest degree which is $\tau(n) - 2$. Since SAEFG is a simple graph so there is no loop at any vertex in particular there is no loop at vertex n itself. Since there are $\tau(n)$ possible vertices of DAFTG. Also, each $d_i \neq 1$ for each i is adjacent to n (possibly). These d_i are $\tau(n) - 2$ in number (excluding 1 and n), so d must have degree $\tau(n) - 2$.

Theorem 2.1. DAEFG is connected and 1 is the only isolated vertex in it.

Proof: Let d_1, d_2, \dots, d_n all the possible divisors of any positive integer n , where $d_n = n$. Since 1 divides each integer, then $a \in \mathbb{V}$. By definition $(1, d_i) = 1$, So 1 cannot join any of the node which means that node 1 is isolated. Now, its only need to show that \mathbb{G} is connected. Since each d_i divide n and which is not co prime to n i.e., $(d_i, n) \geq 1$. So, clearly there is an edge between each d_i to n . Hence, \mathbb{G} is connected.

Proof. The proof is simple. Since, the node 1 is isolated which clearly depicts that no other node can have an edge with node 1. So, there are total $\tau(n) - 1$ nodes in the connected part of graph. As by definition graph is simple so there is no loop. So, there are $\tau(n) - 2$ total number of possible edges incident with node n . Hence, it is the only node with the largest degree which is $\tau(n) - 2$. Since, SAEFG is a simple graph so there is no loop at any vertex in particular there is no loop at vertex n itself. Since there are $\tau(n)$ possible vertices of DAFTG. Also, each $d_i \neq 1$ for each i is adjacent to n (possibly). These d_i are $\tau(n) - 2$ in no. (excluding 1 and n), so d must have degree $\tau(n) - 2$.

Theorem 2.2. \mathbb{G} is always complete for $n = 2^k$.

Proof: Since, $\{1, 2, 2^2, 2^3, \dots, 2^k\}$ be the set of all possible nodes. As $\deg(1) = 0$ so node 1 is not adjacent with any other node. By definition of

τ there are $k + 1$ total possible divisors. By excluding node 1 there are k total possible nodes. Since node 2 is even and each node is of the power of 2 which is again an even number so each node is adjacent to the node 2^k which is the required n . Since the graph is simple so there is neither a loop nor a multi-edge. As each node is adjacent to every other node except itself and the node 1. Hence there are $k - 1$ total possible edges for each node, which is the property of a complete graph by definition.

Lemma 2.1. The graph \mathbb{G} is bipartite for n be the product of two distinct primes.

Proof: The proof can be viewed using its definition. For $n = pq$ then $V = \{1, p, q, pq\}$ be the set of nodes. Since, node 1 is isolated and we take the set of nodes excluding node 1 for the connected part of graph. So, the set of nodes can be split into two disjoint sets as U and V such that $U = \{p, q\}$ and $V = \{pq\}$ with vertex 1 as isolated. As $(p, pq) \geq 1$ and $(q, pq) \geq 1$ but $(p, q) = 1$, so there are edges as $p - pq$ and $q - pq$, where there is no edge between p and q .

Corollary 2.4. There does not exist any cycle for \mathbb{G} for $n = 2^k$.

Theorem 2.3. Let \mathbb{G} be a DAEFG and for $n = p^k q^k, k \geq 2$, then there exist a cycle of length $\tau(p^k q^k) - 1$.

Proof: We will prove this by using increasing powers of these distinct primes. For $n = p^2 q^2$, by definition of DAEFG, $1, p, p^2, q, q^2, pq, p^2 q, pq^2, p^2 q^2$ are the vertices of G . Since, $\tau(n) = 9, (1, p_i) = 1$, It is easy to note that the set $\{p, p^2, q, q^2, pq, p^2 q, pq^2, p^2 q^2\}$ are the only vertices which can contribute a cycle as these vertices are not relatively prime to each other.

$$(p, p^2), (p^2, pq), (pq, p^2 q), (p^2 q, pq^2), (pq^2, q), (q, q^2), (q^2, p^2 q^2), (p^2 q^2, p) \approx C_8.$$

In this way, the powers of n can be taken up to k times. Also, there is no other possible edge with 1 as isolated node. Hence, we have a cycle of length $\tau(p^k q^k) - 1$.

Theorem 2.4. There exists a cycle of length $\tau(p^k q^k r^k) - 1$ in \mathbb{G} for $= p^k q^k r^k, k \geq 2$.

Proof: The proof is a simple consequence Corollary 2.2.

Theorem 2.5. There exist a cycle of length $\tau \left(\prod \left(p_{k_i}^{k_r} \right) - 1 \right)$ in for \mathbb{G} for $n = p_1^{k_1} p_2^{k_2} p_3^{k_3} \dots \dots \dots p_r^{k_r}$ where $p_1 < p_2 < p_3 \dots < p_r$. (Generalized)

Proof. The proof is obvious.

Definition 2.1. A subgraph \mathbb{H} of \mathbb{G} is called is called so it is itself a divisor anti-Euler function graph.

Example 2.1. Let $G(d(\phi'(16)))$ be a DAEFG with vertex set $\mathbb{V} = \{1, 2, 4, 8, 16\}$, then $\mathbb{H}(d(\phi'(8)))$ with vertex set $\mathbb{V} = \{1, 2, 4, 8\}$ is a subgraph of G . Also, both \mathbb{H}_1 and \mathbb{H}_2 are both DAEFG's.

Remark 2.1. It is obvious that each \mathbb{H} is itself \mathbb{G} .

Theorem 2.6. \mathbb{G} is regular for $n = 2^k$, irregular otherwise.

Proof: Let $n = 2^k$ for \mathbb{G} then by definition of \mathbb{G} , $\mathbb{V} = \{1, 2, 2^2, 2^3, \dots, 2^k\}$ be the set of nodes. Also, $(1, 2^i) = 1$ which gives that 1 is not adjacent with any of the nodes among the set of nodes, i.e., 1 is isolated. Since, 2 is even and each of its power is again even i.e., $(2^i, 2^j) \geq 1$ also 2^k is again even, which gives that each node is adjacent to every other node which yield that \mathbb{G} is a complete graph. Also, degree of each node is same in the connected component of \mathbb{G} . By using the result of completeness \mathbb{G} is also regular for $n = 2^k$. Let G be DAEFG, to show that G is regular, each of its vertices should have the same degree.

Theorem 2.7. \mathbb{G} is planar except for $n = 2^k, k \geq 5$.

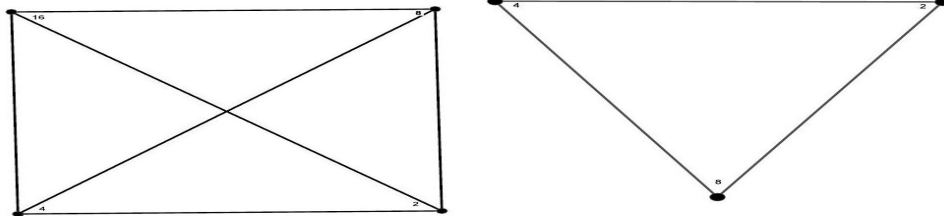


Figure 2. DAEFSG for $n = 8$ and $n = 16$

Theorem 2.8. \mathbb{G} is not Eulerian for any n .

Proof: For $n \geq 3$, (i) if $n = p, \tau(n) = 2$, and $D(n) = \{1, p\}$. Using definition there is no edge between node 1 and the p which gives a null graph. (ii) Secondly, if it is not prime then it is a composite number, which can be even or odd. (i) Suppose that it is even then, $\tau(n) = 2m$ i.e

$\deg(1) = 0$ which shows that node 1 is not adjacent with any of the nodes so the max possible degree of other nodes can be $\deg(d_i) = \tau(n) - 1 \forall d_i \in d(n)$, which is not even, which contradicts the necessity condition for Eulerianity of a graph to have even degree, which gives that \mathbb{G} is not Eulerian. (ii) On the other hand suppose that n is odd, then there are following possibilities. (i) If $\tau(n) = \text{even}$ using above statement, the result is obvious. (ii) But, if $\tau(n) = \text{odd}$, we have all nodes of degree odd in number and no such trail passing via all edges, which is the required result.

Theorem 2.9. \mathbb{G} is Hamiltonian for all $n = p_1^{k_1} p_2^{k_2} p_3^{k_3} \dots p_r^{k_r}$ for $p_1 < p_2 < p_3 \dots < p_r \forall k_i \geq 2$.

Proof. We will prove this result by definition. For any simple \mathbb{G} with more than 3 nodes $\deg(d_i) + \deg(d_j) \geq n$ for every pair of non linked nodes d_i and d_j then \mathbb{G} is Hamiltonian. Now, for $k = 2$, we have $n = p^2 q^2 d(n) = \{1, p, p^2, q, q^2, pq, p^q, pq^2, p^2 q^2\}$, $\tau(n) = p$, Also $\deg(1) = 0$, so other remaining 8 vertices constitute the graph DAEFG, so $\deg(p) + \deg(q) = 10 \geq n$, since p and q are disjoint vertices, i.e. $(p, q) = 1$. Hence, is the result. For $k = 3$, we have $n = p^3 q^3$, then by definition of DAEFG $1, p, p^2, p^3, q, q^2, q^3, pq, p^2 q, p^3 q, pq^2, pq^3, p^2 q^2, p^2 q^3, p^3 q^2, p^3 q^3$, are the vertices. Hence $\tau(n) = 16$. and $\{p, p^2, p^3, q, q^2, q^3, pq, p^2 q, p^3 q, pq^2, pq^3, p^2 q^2, p^2 q^3, p^3 q^2, p^3 q^3\}$ be the nodes that contribute in the construction of DAEFG. Using Dirac theorem the result is again true. It is clear that the result seems true for any of distinct primes with generalized powers up to r , which is the required result. Secondly, if $n = p^k$ and $\tau(n) = \text{even}$ also $\deg(1) = 0$ and $\tau(n) - \{1\}$ nodes form complete graph, which is nowhere Hamiltonian.

Remark 2.2. $\mathbb{G}(p)$ is always a null graph.

Corollary 2.5. $L(\mathbb{G})$ is connected.

Theorem 2.10. \mathbb{G} is $\tau(n) - \{1\}$ for $n = p^k$.

Proof: Since, G be a DAEFG and using its definition Let G be DAEFG, then by definition of $D(n) = \{1, p, p^2, p^3, \dots, p^k\}$ be the set of nodes, and $\tau(n) = k + 1$. As node 1 is not adjacent with any node i.e., $\gcd(1, p^i) = 1$. So, in order to color connected part of graph, we need least number of colors to assign to its nodes. For this, if we 1 to node p , 2 to node p^2 as $(p, p^2) > 1$, 3 to node p^3 , up to node p^k . There are exactly k colors

required to color the set of nodes as $\gcd(p^i, p^j) \geq 1$, which is the required result.

Corollary 2.6. Proof that $\chi(\mathbb{G}(p^k)) = \tau(n) - 1$.

Proof: The proof is a simple consequence of previous theorem that \mathbb{G} is k colorable for p^k as exactly k colors are needed to color its set of nodes. Also, it is the least number of possible such coloring.

Theorem 2.11. \mathbb{G} is $\tau(n) - \{1\}$ -colorable for any $n = p_1^{k_1} p_2^{k_2} p_3^{k_3} \dots p_r^{k_r}$ for $p_1 < p_2 < p_3 \dots < p_r$.

Proof: Since all primes are relatively prime among each other i.e., $(p_i, p_j) = 1$ so, they all can be granted with the same color. But it is essential to see that $\deg(p, p^{k_i}) \geq 1$. In order to grant separate colors to the adjacent nodes, we need r colors as they are in power. Node 1 is in the other part of graph so it can be given among any of the granted color. Also, $|D(n)| = |\tau(n)|$ then, $\tau(n) - \{1\}$ nodes are in the connected part of \mathbb{G} . So, $\chi(\mathbb{G}) = \tau(n) - (r + 1)$.

Corollary 2.7. $\chi(\mathbb{G}) = 2$ for $n = p_1 p_2$.

Proof: It can be shown easily via definition i.e., $\tau(n) = 4$. Also, $(p_1, p_2) = 1$. By Lemma 2.6 depicts that $\mathbb{G} \approx K_{x,y}$ for $n = p_1 p_2$. Also, $\chi(K_{x,y}) = 2$ which is the required result.

Proof. By using the definition of \mathbb{G} , $D(n) = \{1, p\}$. Also, $\gcd(1, p) = 1$ and $\mathbb{G} \approx N$. In this case, exactly one color is sufficient to give both of the nodes in order to color \mathbb{G} .

Theorem 2.12. $\chi'(\mathbb{G}) = k$ for $n = 2^k$.

Proof: Since, the graph has exactly 2 components with 1 as isolated and $1, p, \dots, p^k$ are the τ possible divisors of n . Since, $\tau(n) - \{1\}$ vertices constitute $K_{x,y}$ with even cardinality. As all prime powers are not relatively prime to each other so they are adjacent via edges, so there is no other option but to assign them with a different color. By assigning distinct color to each edge, $\tau(n) - \{1\}$ colors are needed, which is the required result.

Corollary 2.8. $\chi'(\mathbb{G}) = 2$ for $n = p_1 p_2$.

Proof: As proved earlier in Lemma 2.6 i.e., $G \approx K_{x,y}$ for $n = p_1 p_2$. Using definition of $K_{x,y}$, then its max degree δ then $\chi'(\mathbb{G}) = \delta$. As $D(n) = \{1, p_1, p_2, p_1 p_2\}$ be the set of nodes and using definition of DAEFG any two nodes are adjacent to each other if $\gcd(u, v) > 1$. Then, node $(p_1 p_2)$ is the only node with the max degree which is exactly 2. So, $\chi'(\mathbb{G}) = 2$.

Proposition 2.27. $\chi'(\mathbb{G}) = \chi(L(\mathbb{G}))$.

Proof: Since, χ' be the least possible coloring assigned to edges and $L(\mathbb{G})$ is constructed using edges of \mathbb{G} using nodes and χ is the least possible coloring assigned to nodes. Thus, it can be easily seen that $\chi'(\mathbb{G}) = \chi(L(\mathbb{G}))$.

Proposition 2.28. For $n = 2^k$, $D(n) = \{1, 2, 2^2, 2^3, \dots, 2^k\}$ and 1 be the isolated node. Using definition of clique, we need a subset of $D(n)$ for all 2 nodes meet themselves. As $\gcd(2, p_i) = 1$, there exist a graph on $\tau(n) - 1, p$ no. of nodes. So, in this way the largest possible clique can be $\tau(n) - 2$. For a particular case the graph of DAEFG for $n = 36$ is shown below.

Remark 2.3. Here are some useful results regarding DAEFG (i) $D(\mathbb{G}) = 1$ with least dominating set 1. (ii) $\deg(1) = 0$ isolated node. (iii) $\deg_m ax(v) = \tau(n) - 1$ (iv) $O(\mathbb{G}) = 2$ iff $n = p > 2$. (iv) $\deg_m ax(v) = 0$ iff $n = p$ (viii) $g(\mathbb{G}) = 3$

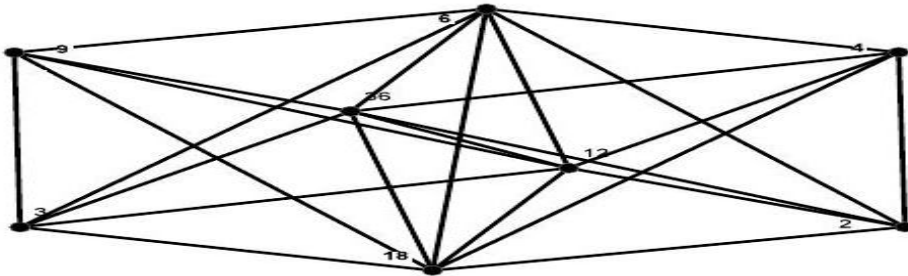


Figure 3. CCC(i), for $i = 1$

3. CONCLUSION

In this work, we have studied the structure of Divisor Anti Euler Function graph DAEFG. We computed its order, degree of nodes, number of components, length of cycle, its subgraphs and other graph theoretic properties. Furthermore, we found chromatic number, chromatic index, Hamiltonicity, Eulerianity, regularity and bipartiteness. In future, we find

DAEFG for any n above discussed graph theoretic properties for arbitrary n .

REFERENCES

1. Kannan K, Narasimhan D, Shanmugavelan S. The graph of divisor function $D(n)$. *Int J Pure Appl Math*. 2015;102(3):483–494. <http://dx.doi.org/10.12732/ijpam.v102i3.6>
2. Mahmood MK, Ali S. On super totient numbers, with applications and algorithms to graph labeling. *Ars Combinatoria*. 2019;143:29–37.
3. Shanmugavelan S. The Euler function graph $G(\varphi(n))$. *Int J Pure Appl Math*. 2017;116:45–48.
4. Babujee JB. Euler's phi function and graph labeling. *Int J Contemp Math Sci*. 2010;5:977–984.
5. Rosen KH. *Elementary number theory*. Pearson Education; 2011.
6. Liu JB, Nadeem MF, Siddiqui HM, Nazir W. Computing metric dimension of certain families of Toeplitz graphs, *IEEE Access*. 2019;7:126734–126741. <https://doi.org/10.1109/ACCESS.2019.2938579>
7. Okamoto F, Phinezy B, Zhang P. The local metric dimension of a graph. *Mathematica Bohemica*. 2010;135(3):239–55. <https://doi.org/10.21136/MB.2010.140702>
8. Feng M, Lv B, Wang K. On the fractional metric dimension of graphs. *Discrete Appl Math*. 2014;170:55–63. <https://doi.org/10.1016/j.dam.2014.01.006>
9. Liu JB, Aslam MK, Javaid M. Local fractional metric dimensions of rotationally symmetric and planar networks. *IEEE Access*. 2020;8:82404–28420. <https://doi.org/10.1109/ACCESS.2020.2991685>
10. Ali S, Mahmood K. New numbers on Euler's totient function with applications. *J Math Exten*. 2019;14:61–83.
11. Mahmood MK, Ali S. A novel labeling algorithm on several classes of graphs. *Punjab Univ J math*. 2017;49:23–35.
12. Harary F, Melter RA. On the metric dimension of a graph. *Ars Combin*. 1976;(191-195):1.

13. Ali S, Ismail R, Campena FJH, Karamti H, Ghani MU. On rotationally symmetrical planar networks and their local fractional metric dimension. *Symmetry*. 2023;15(2):e530. <https://doi.org/10.3390/sym15020530>
14. Mateen MH, Mahmood MK, Ali S, Alam MA. On symmetry of complete graphs over quadratic and cubic residues. *J Chem*. 2021;2021:1–9. <https://doi.org/10.1155/2021/4473637>
15. Mateen MH, Mahmmod MK, Alghazzawi D, Liu JB. Structures of power digraphs over the congruence equation $x^p \equiv y \pmod{m}$ and enumerations. *AIMS Math*. 2021;6(5):4581–4596.
16. Farooq M, Abd ul Rehman A, Mahmood MK, Ahmad D. Upper bound sequences of rotationally symmetric triangular prism constructed as Halin graph using local fractional metric dimension. *VFAST Trans Math*. 2021;9(1):13–27. <https://doi.org/10.21015/vtm.v9i1.1020>
17. Sabahat T, Asif S, Abd ur Rehman A. Structures of digraphs arising from lambert type maps. *VFAST Trans Math*. 2021;9(1):28–36. <https://doi.org/10.21015/vtm.v9i1.1021>
18. Sabahat T, Asif S, Abd ur Rehman A. On fixed points of digraphs over lambert type map. *VFAST Trans Math*. 2021;9(1):59–65. <https://doi.org/10.21015/vtm.v9i1.1023>
19. Ravi V, Desikan K. Brief survey on divisor graphs and divisor function graphs. *AKCE Int J Graphs Combin*. 2023;20(2):217–225. <https://doi.org/10.1080/09728600.2023.2234979>
20. Shanmugavelan S, Rajeswari KT, Natarajan C. A note on indices of primepower and semiprime divisor function graph. *TWMS J Appl Eng Math*. 2021;11(SI):51–62.
21. Antalan JR, De Leon JG, Dominguez RP. On k -dprime divisor function graph. *arXiv preprint arXiv:2111.02183*. <https://doi.org/10.48550/arXiv.2111.02183>
22. Chaudhry F, Husin MN, Afzal F, et al. M-polynomials and degree-based topological indices of tadpole graph. *J Disc Math Sci Crypto*. 2021;24(7):2059–2072. <https://doi.org/10.1080/09720529.2021.1984561>
23. Hameed S, Husin MN, Afzal F, et al. On computation of newly defined degree-based topological invariants of Bismuth Tri-iodide via M-

- polynomial. *J Disc Math Sci Crypto*. 2021;24(7):2073–2091. <https://doi.org/10.1080/09720529.2021.1972615>
24. Ghani MU, Campena FJ, Pattabiraman K, Ismail R, Karamti H, Husin MN. Valency-Based indices for some succinct drugs by using m-polynomial. *Symmetry*. 2023;15(3):e603. <https://doi.org/10.3390/sym15030603>
25. Imran M, Khan AR, Husin MN, Tchier F, Ghani MU, Hussain S. Computation of entropy measures for metal-organic frameworks. *Molecules*. 2023;28(12):e4726. <https://doi.org/10.3390/molecules28124726>
26. Javaid M, Alamer A, Sattar A. Topological aspects of dendrimers via connection-based descriptors. *CMES-Comput Mod Eng Sci*. 2023;135(2):1649–1667. <https://doi.org/10.32604/cmes.2022.022832>
27. Sattar A, Javaid M, Bonyah E. Computing connection-based topological indices of dendrimers. *J Chem*. 2022;2022:e7204641. <https://doi.org/10.1155/2022/7204641>
28. Sattar A, Javaid M, Alam MN. On the studies of dendrimers via connection-based molecular descriptors. *Math Prob Eng*. 2022;2022:1–13.

Scientific Inquiry and Review (SIR)

Volume 7 Issue 4, 2023


ISSN (P): 2521-2427, ISSN (E): 2521-2435

Homepage: <https://journals.umt.edu.pk/index.php/SIR>



Article QR



- Title:** Investigating the Impact of Environmental Toxicology of Heavy Metals in Fish: A Study of Rivers of Pakistan
- Author (s):** Ahmad Manan Mustafa Chatha¹, Saima Naz², Syeda Saira Iqbal³, Unab Zahra¹
- Affiliation (s):** ¹Government Sadiq College Women University, Bahawalpur, Pakistan
²The Islamia University of Bahawalpur, Pakistan
³University of Management and Technology, Lahore, Pakistan
- DOI:** <https://doi.org/10.32350/sir.74.05>
- History:** Received: June 8, 2023, Revised: September 11, 2023, Accepted: November 12, 2023, Published: October 30, 2023
- Citation:** Chatha AMM, Naz S, Zahra U, Iqbal SS. Investigating the impact of environmental toxicology of heavy metals in fish: a study of rivers of Pakistan. *Sci Inq Rev.* 2023;7(4):67–90. <https://doi.org/10.32350/sir.74.05>
- Copyright:** © The Authors
- Licensing:**  This article is open access and is distributed under the terms of [Creative Commons Attribution 4.0 International License](https://creativecommons.org/licenses/by/4.0/)
- Conflict of Interest:** Author(s) declared no conflict of interest



UMT

A publication of
The School of Science
University of Management and Technology, Lahore, Pakistan

Investigating the Impact of Environmental Toxicology of Heavy Metals in Fish: A Study of Rivers of Pakistan

Ahmad Manan Mustafa Chatha¹, Saima Naz², Syeda Saira Iqbal^{3*}, and Unab Zahra¹

¹Department of Zoology, Government Sadiq College Women University, Bahawalpur, Pakistan

²Department of Entomology, Faculty of Agriculture and Environment, The Islamia University of Bahawalpur, Pakistan

³University of Management and Technology, Lahore, Pakistan

ABSTRACT

The global concern of heavy metal toxicity has affected all nations, as the discharge of agricultural runoff and untreated industrial waste into water bodies, including rivers, leads to environmental toxicology. This increased level of heavy metals poses risks not only for marine life but also to those who consume them. While fish is an important protein source, consuming contaminated fish containing high levels of heavy metals can have severe adverse effects on human health. Therefore, it is crucial to address these pollution sources effectively in Pakistan, where a significant portion of the population relies on agriculture and fishing for their living. The country's rapid industrialization and urbanization have substantially increased pollutants in its rivers and other water bodies. The current body of research has indicated that the elevated levels of heavy metals in the ecosystem, including the Indus River, pose a significant threat to the local ecosystem and the well-being of marine life. Heavy metal pollution in Pakistani rivers originates from multiple sources, such as industrial effluents, agricultural runoff, and municipal waste. The unregulated discharge of industrial waste into rivers is a major contributor to heavy metal pollution in Pakistani rivers. Moreover, the excessive and uncontrolled use of fertilizers and pesticides in agriculture equally contributes to the contamination of rivers with heavy metals. The current study is a review article, which provides a comprehensive explanation of how environmental toxicology affects the ecosystem, especially concerning the rivers of Pakistan.

Keywords: contaminated fish, environmental toxicology, fish, river, heavy metals, uncontrolled pollution

* Corresponding Author: saira.iqbal@umt.edu.pk

1. INTRODUCTION

Over the last few decades, water has become a matter of concern for the developing countries. Among many other organic and inorganic pollutants our rivers are getting contaminated with environmental toxicology, creating a harmful impact on the aquatic life. Particularly, this aquatic system has various uses, which are used for sawmills and sand mining, as well as, for daily life activities, such as bathing, washing, and sanitation [1]. Anthropogenic activities pose negative impact on natural water bodies. Heavy pollutants that are discharged from homes, businesses, and industries, may have a negative impact on the river's capacity to provide clear and fresh drinking water, which is essential to serve as a habitat for the ecosystems. Fish are commonly employed as bio-indicators to evaluate the contamination level in the aquatic environment [2]. Ngugi and Oyoo-Okoth [3] asserted that up to 80% of plant protein concentrates an organic form of Cr that can be substituted for fishmeal. The decline in fish populations and fisheries could have an adverse impact on the overall population growth and economic factors [4]. Since fish is a significant source of protein, it's critical to ensure its safety and superiority for better fish production. Since eating contaminated fish can have negative health effects, heavy metal contamination in fish has received extensive research on a global scale [5]. Since it contains omega-3 fatty acids, DHA, and EPA, fish offers a complete dietary package of energy, protein, amino acids, vitamins, and minerals. Moreover, fish has also been linked to positive health effects like protection against diabetes and cardiovascular diseases. Furthermore, fish's health benefits were negated (cancelled) by contamination, and consumers may experience health risks [6]. As it is used as food, Southeast Asian countries frequently cultivate the Indian major carp *Cirrhinus mrigala*, also known as the Mrigal fish [7]. Monitoring the amount of heavy metals in Mrigal fish is crucial because eating tainted Mrigal fish could be harmful to one's health [8]. According to scientific knowledge, the presence of toxic metals in aquatic ecosystems has detrimental properties on the organisms inhabiting them due to their persistent nature and tendency to accumulate. Sub-lethal effects resulting from heavy metal pollution or toxicology can significantly affect the long-term growth, reproductive capabilities, and overall survival of organisms in the ecosystem. [9]. The following metals are indicated below, which are poisonous for the fish species and ecosystem.

1.1. Cadmium

The aquatic environment and the crust of the Earth both contain significant concentrations of cadmium, a highly toxic heavy metal that has a detrimental effect on fish survival, development, and reproduction\Cd accumulation in fish tissues, particularly the kidneys, liver, and gills, which can result in a number of physiological and structural issues [10]. Fish are the primary predators in aquatic ecosystems, making them particularly susceptible to Cd pollution. The accumulation of Cd in their tissues may negatively affect their gills, liver, gonads, and other organs, which may cause problems with their metabolism, physiology, and reproduction, as well as, cause death [11]. Within aquatic environments that have been contaminated with cadmium (Cd), fish can experience stress due to the presence of ROS (reactive oxygen species) and RNS (ribonucleic acid enzymes) [12].

1.2. Lead (Pb)

Lead (Pb) is a compound that is found at low concentrations in the crust of the earth, predominantly as sulfide. The origins of lead emissions differ significantly based on their location and stages. However, on a country-wide scale, the primary contributors to airborne lead are the processing of ores and metals, as well as piston-engine aircraft that utilize leaded aviation fuel. Other significant contributors include waste incinerators, utilities, and manufacturers of lead-acid batteries. Generally, the air around lead smelters contains the most concentrated levels of lead. Depending on the dosage, lead (Pb), a heavy metal with toxic effects on health, can cause a wide range of negative effects. The developing central nervous system (CNS) is more susceptible to toxicity from Pb than other organ systems. Children are more susceptible to Pb toxicity when compared to adults because of the increased hand-to-mouth activity and intestinal absorption. In children and adults, it can cause several health problems, including renal failure, and coma, ultimately leading to death. Pb is considered a non-essential component, which is widely recognized due to its toxicity, which can lead to nephrotoxicity, neurotoxicity, and various detrimental impacts [13]. Trash fish used in the production of feed may have contributed to the high Pb levels found in fish feed and cultured tilapia. The results of the study indicated that the majority of the samples of raw, tank, and tap water from the lakes of Darbandikhan and Dokan, which were tested between June 2012 to May 2013, for a few water safety parameters had high levels of

heavy metals like Cd and Pb, exceeding the thresholds advised by the WHO and FAO organizations.

1.3. Nickel

The chemical element nickel (Ni), which makes up about 3% of the Earth's crust, is naturally distributed in the air. Along with iron, cobalt, palladium, platinum, and five other elements, it is a part of group VIII B of the periodic table and a member of the transition series. Despite being common, nickel is harmful to living things. However, it is released into the air through fossil fuels and other various natural and anthropogenic activities. A study conducted [14] indicated that red blood cells (RBC) of *Cirrhinus mrigala* exposed to sub-lethal nickel concentrations showed a reduction in RBC count. It was also discovered that there was a correlation between nickel concentration and fish mortality. One of the natural sources of atmospheric nickel is wind-borne dust from soil and rock weathering, volcanic emissions, vegetation, and forest fires. Most anthropogenic sources of nickel in the environment are both stationary and mobile, including burning coal, diesel, and fuel oil as well as sewage, waste, and other materials [15]. Several prior studies have discussed the hazardous effects of Ni, which are highly reported in the urban atmosphere.

1.4. Copper

Copper is an essentially significant element, which is present in dietary products. Copper (Cu) acts as an enzyme that reduces the molecular oxygen by creating approximately a tolerable intake level. The majority of the organisms regulate copper, a vital element required for hemoglobin synthesis and for the functioning of numerous enzymes. However, research has shown that aquatic life, such as fish, invertebrates, and amphibians, can be extremely toxic to copper (Cu) and are all equally sensitive to chronic toxicity [16]. Organs of fish and mollusks frequently accumulate copper. Lamellae fusion has been associated with chronic copper exposure, whereas aneurysms and edema have been associated with short-term copper exposure [17]. Due to their direct exposure to water, fish gills are the initial organs to respond to environmental pollution, making them highly susceptible to the detrimental impacts of copper accumulation. Copper can also change the cellular makeup, glucose metabolism, and salt balance of fish. Due to fish efficiency bioaccumulators and heavy metals like copper can easily accumulate in their tissue, which could be harmful to human

For instance, [20] Yang, Hu [21] 's recent research on crucian carp found that exposure to cadmium interfered with the ion transport mechanisms in the fish's gills, impairing osmoregulation and acid-base balance. Furthermore, heavy metals can disrupt various biochemical pathways in fish production by interfering with their enzymatic functions. For instance, the enzyme acetylcholinesterase, which is essential for the proper functioning of fish nerves, can be inhibited by lead, as indicated by the recent investigation by [22] . (See Figure1).

3. HEAVY METAL EFFECT ON EMBRYONIC DEVELOPMENTAL OF FISH

According to [23], environmental pollutants, including waterborne metals have detrimental effects on fish embryos and larvae, which are considered the life stages with most vulnerable and toxic impacts. The presence of metals in the water can interfere with the development of fish embryos, potentially leading to adverse outcomes. Numerous studies have demonstrated that heavy metals can have a negative impact on developing fish production, especially in their embryonic and larval stages, causing high mortality rates, delayed hatching, abnormal body shape, and physical anomalies [24]. The effects resulting from heavy metal exposure encompass several detrimental outcomes, such as stunted growth rate, delayed and diminished hatching, reduced survival rates of embryos and larvae, and hatching that is both reduced and delayed. A recent study indicated that heavy metal toxicity specifically affects marine fish embryos and larvae, leading to reduced hatchability [25]. Much research has been conducted to investigate the toxic effects of these heavy metals on fish embryos and larvae, resulting in a substantial body of literature on this topic. For instance, zebrafish embryos exposed to cadmium concentrations similar to those tested in the current study from the gastrula stage onwards manifested a definite delay in hatching. Additionally, the newly emerged larvae had diminished swimming abilities [26].

3.1. Effect Fish Production

It has been noted that the buildup of toxic substances causes aquatic organisms, including fish, to experience a decline in growth and reproduction. Fish deformities can alter a fish's chances of surviving, thus, leading to the decline rate of growth, welfare, and external morphology, all of which can have a devastating impact on populations. Deformities of the

vertebral column are among the most frequently described fish deformities in the literature [24]. Fish exposure to sub-lethal levels of metal mixtures can have detrimental effects on the overall fish growth and health. Metal mixtures can have a wide variety of effects on fish. Fish species' responses to food intake, food conversion efficiency, weight increments, and length increments, were discovered to be significantly different due to their exposure to metal mixtures, indicating significant effects on their growth [27]. In treated fish species, weight and fork/total lengths were found to be negatively correlated and statistically significant, while in control fish species, the correlation was positive but not statistically significant, [28, 29]. The study revealed a significant and positive correlation between weight gains, condition factors, and feed intake in both the treated and control fish species. This observation emphasized the link between fish condition and the quantity of feed consumed, which impacts the degree of weight gain. The study specifically focused on grower pond cultures of *Cirrhina mrigala*, *Labeo rohita*, and *Catla catla* [30] a long-term impact on growth, net fish production, and yield when fingerlings were exposed to lead (Pb) at sub-lethal concentrations. The study determined that the growth and yield of the fish species were adversely affected by sub-lethal lead exposure. This conclusion was based on observations of reduced weight gain, fork, and total length gains, as well as a decrease in net fish production [31, 32]. The study examined how the chemical properties of water can influence the growth capacity of *Ctenopharyngodon idella* and *Hypophthalmichthys molitrix* under sub-lethal stress as induced by a mixture of metals. The findings further also revealed that the growth of both fish species was significantly affected by the physico-chemical characteristics of the stressed media [31].

3.2. Removal of Heavy Metals

To keep the environment clean and boost human health, heavy metal ions must be successfully removed from wastewater. Numerous techniques, such as electrocoagulation, adsorption using synthetic and natural materials, the use of magnetic fields, sophisticated oxidation techniques, membranes, and others, have been developed to deal with this issue [33, 34]. According to Zhang and Hou [35], the sequential extraction method facilitates the understanding of metal movement in soil and groundwater. Physical remediation techniques, such as washing, soil extraction, solidification, and stabilization offer viable means of removing heavy metals from soil.

However, among the various methods available, adsorption is considered the maximum capable approach for the elimination of toxic metals. This is mainly because of its high effectiveness, broad pertinence, and its cost-effectiveness. Iron Magnesium oxides have become a commonly utilized adsorbent due to their simple preparation, abundant availability of raw materials, and minimal environmental impact. Regarding the deletion of these toxic metals from solutions, the main methods include ion exchange utilizing iron-manganese oxide nanomaterials and redox reactions. Further research is needed in these areas to enhance our understanding and optimize the utilization of these materials for effective removal of heavy metals [36]. Various physical techniques like ultrafiltration, coagulation, flocculation, adsorption, membrane filtration, and ion exchange are employed for heavy metal removal from water. Chemical strategies encompass neutralization, solvent extraction, chemical precipitation, and electrochemical treatment. A number of these methods are commonly adopted for the removal of heavy metals from water. These methods can be used individually or in combination depending on the specific situation and the types and levels of heavy metals, which are required to be removed. Each method has its own benefits and drawbacks and the choice of method would depend on a variety of factors including its cost, effectiveness, and environmental impact [37].

4. HEAVY METAL POLLUTION IN RIVERS OF PAKISTAN

According to the provided sources, the deterioration of the Indus River and other wetlands in Pakistan has resulted in heightened health hazards for the nearby communities. Although aquatic systems are vital sources of freshwater for the ecosystems that support all forms of life, their deteriorating water quality poses a severe threat to their long-term survival. Globally, rivers play a pivotal role as critical waterways, serving as the primary source of the water resources that are being utilized for agricultural, industrial, and domestic purposes [38, 39].

Ali, Khan [40] ensuring the well-being of the aquatic ecosystem necessitated diligent monitoring of river water quality. Furthermore, evaluating the concentration of these toxic metals in fish species is of utmost importance because of their significant role in the human diet and the potential risks they pose to public health [41]. The River Shah Alam, located in Khyber Pakhtunkhwa, Pakistan, has faced pollution issues caused by the release of many toxic industrial sewages, agricultural runoff, and local mess from Peshawar and its surrounding areas. Previous studies have

demonstrated that sub-lethal exposure to lead (Pb) can negatively impact the immune systems of tilapia fish (*Oreochromis mossambicus*). By assessing the effects of these toxic metals, the study aimed to gain insights into the potential contamination and associated risks for the aquatic ecosystem and the fish inhabiting the river. The river systems in Pakistan have been adversely affected by the excessive discharge of metallic compounds, resulting in a decline in freshwater fisheries specifically in the river Ravi [42]. The release of effluents into lakes resulting from rapid urbanization and industrialization is a significant global issue, contributing to the presence of various toxic pollutants in the aquatic environment. Among these pollutants, heavy metals are particularly concerning due to their persistent nature and the potential for biological accumulation [43]. Water bodies like rivers, lakes, and oceans are frequently subjected to the disposal of heavy metals, which can subsequently accumulate in fish through multiple routes, including ingestion, skin contact, and gill absorption. As a result, fish can accumulate these traces of heavy metals at significantly higher levels than their concentrations in the surrounding water. The accumulation of heavy metals in fish through the process of bioaccumulation presented a potential hazard to both aquatic ecosystems and human well-being [44]. The increased concentrations of nickel (Ni) found in water samples taken from three rivers in District Charsadda, Khyber-Pakhtunkhwa, Pakistan, are attributed to the discharge of effluents originating from pharmaceutical industries [45]. The Faisalabad city, in Pakistan is a major contributor to this pollution, as it releases both industrial and municipal waste into the river through the Chakbandi drain. Consequently, the river exhibits high pollution levels, resulting in reduced water productivity and a significant increase in the bioaccumulation of pollutants in the muscle tissues of fish, particularly in the case of *Cirrhinus mrigala*. Elevated levels of heavy metals have detrimental effects on the overall well-being of fish, leading to disruptions in their normal physiological processes [46]. A recent investigation conducted on the Panjkora River yielded similar findings, demonstrating elevated concentrations of heavy metals in fish organs [47]. Factors such as age, sex, size, diet, and movement patterns can all contribute to metal accumulation in fish. Additionally, environmental factors like pH, temperature, calcium concentration, and water hardness can also impact metal accumulation. Unregulated disposal of industrial and agricultural waste, rapid urbanization, and population growth are the leading causes of water

pollution [48] as per the citation, the Swat River is a significant source of water for the Swat district that begins in the mountains (glaciers) of Kalam before running longitudinally through the Swat district and entering the Dir district at Chakdara. In the study conducted along the River Swat, which harbors valuable fish species like *Oncorhynchus mykiss* and *Shizothorax esocinus*, the prime objective was to evaluate the presence of heavy metal contamination in different environmental components, such as water, sediments, algae, and fish tissues. The research revealed that *Graptophyllum reticulatum*, in particular, exhibited higher concentrations of heavy metals in its muscles, skin, liver, and gills as compared to *Cyprinus carpio*. The accumulation of these metals within fish cells poses a potential risk of fish mortality [49]. The release of untreated industrial wastewater into rivers and streams is a significant concern in Pakistan, leading to freshwater pollution. Shockingly, approximately 99% of industrial wastewater is discharged without undergoing any form of treatment [50]. A startling revelation was uncovered concerning the amount of lead (Pb) found in fish samples. The research results indicated that both 90% of the fish procured from the main market and every sample taken from retail shops, exceeded the international acceptable limit of 0.123g for lead content. This revelation is profoundly agonizing, as high lead concentrations in fish not only present health hazards to consumers but also to the fish farmers engaged in the cultivation process [51]. In this study, the bioaccumulation of lead (Pb) and cadmium (Cd) in the gills, swim bladders, and muscle tissues of *Tor putitora* fish species were examined. The species (fish) samples were collected from three sites in District Swabi, Khyber Pakhtunkhwa, Pakistan (Batakra, Ghazi, and Kund) between February and April 2016 [52]. (See Table 1)

Table 1. Heavy Metal Pollution in River of Pakistan

Fish species/ Water samples	Location	Metals	Method	Effect	References
<i>Cirrhina mrigala</i> ,	Baloki Headworks	Cd, Cr	Bioaccumulation in fish organ by flame atomic absorption spectrophotometer	Fish liver exhibited the highest tendency to accumulate both cadmium and chromium, while the accumulation of both metals was the minimum in fish gills.	[42]
Water samples	River Kabul	Cu,Cr, Ni, Pb, Cd	Bioaccumulation AAS	This affects the growth of the inhabitant fish population and in turn productivity of the river.	[53]
<i>Cyprinus carpio</i> ,	Nandana River,	Cu, Cr, Fe, Ni, Pb	Bioaccumulation by flame atomic absorption spectrophotometer	Oxidative stress is brought on, which harms the cellular structure of body organs. No metal was discovered to individually present a risk to non- cancerous health.	[54]
<i>Schizothorax plagiostomus</i>	River Panjk	Cu, Pb, Cr, Ni, Cd	Bioaccumulation in fish organ by flame atomic absorption spectrophotometer	Bioaccumulation of nickel (Ni) in fish muscles, the elevated concentrations of Ni found in the fish samples may be attributed to the introduction of this metal into the river waters.	[55]
<i>Schizothorax plagiostomus</i>	River Swat	Pb, Cr, Ni, and Zn	Bioaccumulation atomic absorption spectrophotometer.	<i>Schizothorax plagiostomus</i> exhibits the highest accumulation of chromium (Cr) in both the gills and muscles	[56]
<i>Glyptothorax punjabensis</i>) <i>Cyprinus carpio</i>	Jindi, Khyali	Cr,Cu,Ni,Mn.Co	Goal Hazard Ratio Atomic absorption spectrophotometer, cancer risk at the target, and danger index.	The calculated cancer risk associated with nickel (Ni) for the given fish species exceeded the accepted risk level. Among the three fish species examined, <i>Cyprinus carpio</i> demonstrated the highest health risk, followed by <i>Glyptothorax punjabensis</i> .	[57]

Fish species/ Water samples	Location	Metals	Method	Effect	References
<i>Tilapia nilotica</i> , <i>Wallago attu</i> , <i>Catla catla</i>	Head Islam (Hasilpur),	Cu, Pb, Cr, Ni, Cd	Bioaccumulation Atomic absorption spectrophotometer	Vacuoles of varying sizes were observed in the affected liver cells, indicating cellular damage. Additionally, cell death, hemorrhage, and rupture of blood cells were observed between the hepatocytes, along with dilation in hepatoportal blood vessels	[58]
<i>Cirrhina mrigala</i>	Indus River	Zn,Ni,Cu	Atomic Absorption Spectrophotometer	The activity of CAT enzyme was higher in kidneys and gills of farm fish compared to the liver of hatchery fish. Variations in antioxidant defense system.	[59]
<i>Schizothorax niger</i>	River Jhelum	Cu ²⁺ , Zn ²⁺ , Pb ²⁺ and Fe ²⁺	Bioaccumulation and biomagnification, Atomic Absorption Spectrophotometer	Fish can be harmful and toxic. In order to harm fish, Cu ²⁺ can actively combine with other substances and elements like ammonia (NH ₃ , Hg, and Zn ²⁺). May result in a reduction in fish fertility.	[60]
<i>Labeo calbasu</i>	Chenab River.	Cr,PB,Zn	Spectrophotometer (model Spectra AA800).	In the liver of CF fish, the activity of superoxide dismutase (SOD), catalase (CAT), glutathione (GSH), and lipid peroxidase (LPO) was observed to be higher compared to HF fish (P < 0.05). Furthermore, the HF fish exhibited higher levels of Cr, Co, Cu, and Fe in their muscle tissues compared to CF fish. As fish muscles are a significant edible portion, these findings raise	[61]

Fish species/ Water samples	Location	Metals	Method	Effect	References
				concerns about the potential health risks for consumers.	
<i>Labeo rohita</i>	Head Balloki	Hg	Atomic fluorescence spectrometer.	Metal buildup results in oxidative stress that is toxic and causes genotoxicity as well as the usual changes in SOD, CAT, and MDA levels.	[62]
<i>Cyprinus carpio</i>	Rawal Lake,	Cd, Co, Cr, Cu, Fe	Flame atomic absorption spectrophotometer	Carcinogenic and non-carcinogenic effects in fish	[63]
<i>Cyprinus carpio</i>	Indus River in Mianwali	(Mn, Pb, Zn, Hg and Cr	Coupled plasma optical emission spectroscopy.	The fish demonstrated higher bioaccumulation of essential metals such as zinc (Zn) compared to toxic metals like lead (Pb). However, the elevated concentrations of manganese (Mn), mercury (Hg), and chromium (Cr) in fish muscles could potentially pose health risks to individuals consuming these fish	[64]
<i>Labeo rohita</i>	River Kabul	Cr,Fe	Atomic Absorption Spectrophotometer	The metals that were most concentrated in both species' gills and livers were chromium and iron.	[65]
<i>Salmo trutta fario</i>	River Swat.	Hg	Using the hydride generation method, an atomic absorption spectrometer (GBC 932 plus).	The fishing community encountered various health problems, including muscle pain, headaches, visual impairment, high arterial blood pressure, anemia, and kidney dysfunction.	[66]

Fish species/ Water samples	Location	Metals	Method	Effect	References
<i>Sarda orientalis</i>	Pakistan (northern Arabian Sea)	Zn Mn,Cu Cd	Atomic Absorption Spectrophotometer	A serious threat to human health is posed by metal contamination in marine fish.	[67]
<i>OREOCHROMIS NILOTICUS</i>	Tarukri Drain	Cd,Fe, Pb, Ni, Zn	Atomic Absorption Spectrophotometer, Bioaccumulation	The kidney, liver, and muscles all had the highest concentrations of heavy metals cause a variety of harms to fish, and its consumers may also be at risk for health problems.	[68]
MASTACEMBELUS ARMATUS	Shah Alam	Cr, Ni, Pb,Cd	AAS	Fish exposed to heavy metals experience pathological changes and a disruption in the release of reproductive hormones. Fish exposed to Cr experience biochemical, haematological, and behavioural changes.	[40]
<i>CYPRINUS CARPIO</i>	SHAHPUR DAM	Pb, Cu, Cr, Fe, Ni)	Atomic absorption spectrophotometer, cancer risk, and hazard index (HI) (CR)	Oxidative stress was assessed using the catalase (CAT), glutathione S-transferase (GST), and reduced glutathione (GSH) activities in the liver and gill of Cyprinus carpio. DNA damage	[54]
C. IDELLA	HEAD PUNJNAD	Cd,Hg	Atomic absorption spectrometer made by Zeeman (Z- 5000, Hitachi Japan).	Damage to the kidney can result in chronic toxicity, which can also cause body tumours, liver dysfunction, poor chances for reproduction, loss of routine kidney functions, and hypertension.	[69]

5. CONCLUSION

This study crucially highlighted that the presence of heavy metals creating environmental toxicology has severely impacted the ecosystem by raising several significant environmental concerns that demand immediate attention. Water bodies, such as rivers, become contaminated due to the release of untreated industrial waste and agricultural runoff containing heavy metals. Fish play a pivotal role in the food chain and can potentially become a source of heavy metal exposure for both aquatic creatures and people who consume them. Addressing this problem requires collaboration among the public, private, and local communities to highlight the need to necessitate to develop sources, which will decrease the industrial effluents and increase fish production. The government should enforce stringent regulations and implement robust monitoring mechanisms to ensure that industries adhere to environmental standards and refrain from releasing hazardous waste into water bodies. In conclusion, the heavy metal analysis conducted in this study addressed the complex issue of contamination of environmental toxicology in Pakistani rivers. Moreover, using the fish sample, it was highlighted that a comprehensive approach involving various stakeholders was required to sustain the fish production and ecosystem. Additionally, it was indicated that by working together, the sustainable utilization of natural resources can be ensured to promote the well-being of the communities. Industrial growth, coupled with poor waste management strategies, has led to a significant degradation in the quality of water bodies. Hence, several key contaminants, including untreated industrial effluents, municipal waste, agricultural runoff, and improperly disposed-of domestic waste, all of which have turned the aquatic systems into repositories of pollutants, increasing the nature of heavy metals and toxins.

In particular, toxic heavy metals and microplastics have been identified as severe threats to both aquatic ecosystems and human health. Their presence has not only disrupted the riverine ecology but also entered the food chain, affecting people and other organisms at higher trophic levels. Moreover, the high levels of organic pollutants have depleted oxygen levels in the water, leading to massive fish die-offs and the destruction of aquatic biodiversity.

REFERENCES

1. Angriani P, Sumarmi, Ruja IN, Bachri S. River management: the importance of the roles of the public sector and community in river preservation in Banjarmasin (A case study of the Kuin River, Banjarmasin, South Kalimantan–Indonesia). *Sustain Cities Soc.* 2018;43:11–20. <https://doi.org/10.1016/j.scs.2018.08.004>
2. Lynch AJ, Cooke SJ, Deines AM, et al. The social, economic, and environmental importance of inland fish and fisheries. *J Physiol Pharmacol.* 2016;24(2):115–121. <https://doi.org/10.1139/er-2015-0064>
3. Ngugi CC, Oyoo-Okoth E, Manyala JO, Fitzsimmons K, Kimotho A. Characterization of the nutritional quality of amaranth leaf protein concentrates and suitability of fish meal replacement in Nile tilapia feeds. *Aquac Rep.* 2017;5:62–69. <https://doi.org/10.1016/j.aqrep.2017.01.003>
4. Limburg KE, Hughes RM, Jackson DC, Czech B. Human population increase, economic growth, and fish conservation: collision course or savvy stewardship? *Fisheries.* 2011;36(1):27–35. <https://doi.org/10.1577/03632415.2011.10389053>
5. You SH, Wang SL, Pan WH, Chan WC, Fan AM, Lin P. Risk assessment of methylmercury based on internal exposure and fish and seafood consumption estimates in Taiwanese children. *Int J Hygiene Environ Health.* 2018;221(4):697–703. <https://doi.org/10.1016/j.ijheh.2018.03.002>
6. Varol M, Kaya GK, Alp A. Heavy metal and arsenic concentrations in rainbow trout (*Oncorhynchus mykiss*) farmed in a dam reservoir on the Firat (Euphrates) River: Risk-based consumption advisories. *Sci Total Environ.* 2017;599-600:1288–1296. <https://doi.org/10.1016/j.scitotenv.2017.05.052>
7. Joardar SN, Abraham TJ, Mandal N. Indian major carp *Cirrhinus mrigala* (Hamilton, 1822) inoculated with live *Aeromonas hydrophila* shows dynamic changes in specific immune-cellular activities. *J Immunol Immunopathol.* 2015;17(1):25–30. <https://doi.org/10.5958/0973-9149.2015.00003.9>
8. Ullah S, Hasan Z, Zuberi A. Heavy metals in three commercially valuable cyprinids in the river Panjkora, district Lower Dir, Khyber

- Pakhtunkhwa, Pakistan. *Toxicol Environ Chem.* 2016;98(1):64–76. <https://doi.org/10.1080/02772248.2015.1100916>
9. Dixit R, Wasiullah X, Malaviya D, et al. Bioremediation of heavy metals from soil and aquatic environment: an overview of principles and criteria of fundamental processes. *Sustainability.* 2015;7(2):2189–2212. <https://doi.org/10.3390/su7022189>
 10. Al-Asghar NA, Abdel-Warith AW, Younis ES, Allam HY. Haematological and biochemical parameters and tissue accumulations of cadmium in *Oreochromis niloticus* exposed to various concentrations of cadmium chloride. *Saudi J Biol Sci.* 2015;22(5):543–550. <https://doi.org/10.1016/j.sjbs.2015.01.002>
 11. Liu Y, Chen Q, Li Y, Bi L, Jin L, Peng R. Toxic effects of cadmium on fish. *Toxics.* 2022;10(10):e622. <https://doi.org/10.3390/toxics10100622>
 12. Rehman T, Naz S, Hussain R, et al. Exposure to heavy metals causes histopathological changes and alters antioxidant enzymes in fresh water fish (*Oreochromis niloticus*). *Asian J Agric Biol.* 2020;2001(1):1–11. <https://doi.org/10.35495/ajab.2020.03.143>
 13. Garcia-Vazquez E, Perez J, Martinez JL, et al. High level of mislabeling in Spanish and Greek hake markets suggests the fraudulent introduction of African species. *J Agric Food Chem.* 2011;59(2):475–480. <https://doi.org/10.1021/jf103754r>
 14. Kumar M, Prabhakar C. Physico-chemical parameters of river water: a review. *Int J Pharma Biol Arch.* 2012;3:1304–1312.
 15. Parthipan P, Muniyan M. Effect of heavy metal nickel on hematological parameters of fresh water fish, *Cirrhinus mrigala*. *J Environ Current Life Sci.* 2013;1:46–55.
 16. Khabbazi M, Harsij M, Hedayati SA, Gerami MH, Ghafari-Farsani H. Histopathology of rainbow trout gills after exposure to copper. *Iran Soc Ichthyol.* 2014;1(3):191–196.
 17. Kamaruzzaman BY, Ong MC, Rina SZ, Joseph B. Levels of some heavy metals in fishes from Pahang river estuary, Pahang, Malaysia. *J Biol Sci.* 2010;10(2):157–161.
 18. Sabullah MK, Sulaiman MR, Shukor MY, et al. The assessment of cholinesterase from the liver of *Puntius javanicus* as detection of metal

- ions. *Sci World J.* 2014;2014:e571094. <https://doi.org/10.1155/2014/571094>
19. Bibi S, Naz S, Saeed S, Chatha AM. A review on histopathological alterations induced by Heavy Metals (Cd, Ni, Cr, Hg) in different fish species. *Punjab Univ J Zool.* 2021;36(1):81–89. <https://dx.doi.org/10.17582/journal.pujz/2021.36.1.81.89>
 20. Katoch S, Patial V, Zebrafish: an emerging model system to study liver diseases and related drug discovery. *J Appl Toxicol.* 2021;41(1):33–51. <https://doi.org/10.1002/jat.4031>
 21. Yang L, Hu W, Chang Z, et al. Electrochemical recovery and high value-added reutilization of heavy metal ions from wastewater: Recent advances and future trends. *Environ Int.* 2021;152:e106512. <https://doi.org/10.1016/j.envint.2021.106512>
 22. Zhang J, Meng H, Kong X, et al. Combined effects of polyethylene and organic contaminant on zebrafish (Danio rerio): Accumulation of 9-Nitroanthracene, biomarkers and intestinal microbiota. *Environ Pollut.* 2021;277:e116767. <https://doi.org/10.1016/j.envpol.2021.116767>
 23. Zhang H, Cao H, Meng Y, et al. The toxicity of cadmium (Cd²⁺) towards embryos and pro-larva of soldatov's catfish (Silurus soldatovi). *Ecotoxicol Environ Saf.* 2012;80:258–265. <https://doi.org/10.1016/j.ecoenv.2012.03.013>
 24. Jezierska B, Ługowska K, Witeska M. The effects of heavy metals on embryonic development of fish (a review). *Fish Physiol Biochem.* 2009;35:625–640. <https://doi.org/10.1007/s10695-008-9284-4>
 25. Taslima K, Al-Emran M, Rahman MS, et al. Impacts of heavy metals on early development, growth and reproduction of fish—A review. *Toxicol Rep.* 2022;9:858–868. <https://doi.org/10.1016/j.toxrep.2022.04.013>
 26. Gouva E, Nathanailides C, Skoufos I, Paschos I, Athanassopoulou F, Pappas IS. Comparative study of the effects of heavy metals on embryonic development of zebrafish. *Aquacul Res.* 2020;51(8):3255–3267. <https://doi.org/10.1111/are.14660>

27. Naeem M, Salam A, Tahir SS, Rauf N. The effect of fish size and condition on the contents of twelve essential and non essential elements in *Aristichthys nobilis*. *Pak Veter J*. 2011;31(2):109–112.
28. Naz S, Javed M. Growth responses of fish during chronic exposure of metal mixture under laboratory conditions. *Pak Veter J*. 2013;33(3):354–357.
29. Al-Saeed FA, Naz S, Saeed MH, et al. Oxidative Stress, antioxidant enzymes, genotoxicity and histopathological profile in *oreochromis niloticus* exposed to lufenuron. *Pak Veter J*. 2023;43(1):160–166.
30. Naz S, Javed M, Hayat S, Abdullah S, Bilal M, Shaukat T. Long term effects of lead (Pb) toxicity on the growth performance, nitrogen conversion ratio and yield of major carps. *Pak J Agricul Sci*. 2008;45(3):53–57.
31. Naz S, Javed M, Tahir A, Azmat H. Impact of physico-chemical variables of test media on growth performance of metal stressed major carps. *Pak J Zool*. 2012;44(5):1291–1296.
32. Naz S, Mansouri B, Chatha AM. et al. Water quality and health risk assessment of trace elements in surface water at Punjnad Headworks, Punjab, Pakistan. *Environ Sci Pollut Res*. 2022;29(40):61457–61469. <https://doi.org/10.1007/s11356-022-20210-4>
33. Qasem NA, Mohammed RH, Lawal DU. Removal of heavy metal ions from wastewater: a comprehensive and critical review. *NPJ Clean Water*. 2021;4:e36. <https://doi.org/10.1038/s41545-021-00127-0>
34. Naz S, Hussain R, Ullah Q, Chatha AM, Shaheen A, Khan RU. Toxic effect of some heavy metals on hematology and histopathology of major carp (*Catla catla*). *Environ Sci Pollut Res*. 2021;28(6):6533–6539. <https://doi.org/10.1007/s11356-020-10980-0>
35. Zhang Q, Hou Q, Huang G, Fan Q. Removal of heavy metals in aquatic environment by graphene oxide composites: a review. *Environ Sci Pollut Res*. 2020;27:190-209. <https://doi.org/10.1007/s11356-019-06683-w>
36. Li M, Kuang S, Kang Y, Ma H, Dong J, Guo Z. Recent advances in application of iron-manganese oxide nanomaterials for removal of

- heavy metals in the aquatic environment. *Sci Total Environ.* 2022;819:e153157. <https://doi.org/10.1016/j.scitotenv.2022.153157>
37. Chatha AM, Naz S, Naz S, Khan RU, Nawaz A. heavy metal pollution in water from anthropogenic and natural activities and the remediation strategies. In: Ahmad MI, Mahamood M, Javed M, Alhewairini SS, eds., *Toxicology and Human Health: Environmental Exposures and Biomarkers*. Singapore: Springer; 2023:27–53. https://doi.org/10.1007/978-981-99-2193-5_2
 38. Zeb BS, Malik AH, Waseem A, Mahmood Q. Water quality assessment of Siffran river, Pakistan. *Inter J Phy Sci.* 2011;6(34):7789–7798. <https://doi.org/10.5897/IJPS11.1385>
 39. Chatha AM, Naz S, Mansouri B, Nawaz A. Accumulation and human health risk assessment of trace elements in two fish species, *Cirrhinus mrigala* and *Oreochromis niloticus*, at Tarukri Drain, District Rahimyar Khan, Punjab, Pakistan. *Environ Sci Pollut Res.* 2023;30:56522–56533. <https://doi.org/10.1007/s11356-023-26337-2>
 40. Ali H, Khan E, Nasir MJ. Bioaccumulation of some potentially toxic heavy metals in freshwater fish of river Shah Alam, Khyber Pakhtunkhwa, Pakistan. *Pak J Zool.* 2020;52(2):603–608.
 41. Kaya H, Akbulut M, Çelik EŞ, Yılmaz S. Impacts of sublethal lead exposure on the hemato-immunological parameters in tilapia (*Oreochromis mossambicus*). *Toxicol Environ Chem.* 2013;95(9):1554–1564. <https://doi.org/10.1080/02772248.2014.895363>
 42. Rauf A, Javed M, Ubaidullah M. Heavy metal levels in three major carps (*catla catla*, *labeo rohita* and *cirrhina mrigala*) from the river ravi, Pakistan. *PakVeter J.* 2009;29(1):24–26.
 43. Akan JC, Mohmoud S, Yikala BS, Ogugbuaja VO. Bioaccumulation of some heavy metals in fish samples from river benue in vinikilang, adamawa state, Nigeria. *Am J Analyt Chem.* 2012;3:727–736. <https://doi.org/10.4236/ajac.2012.311097>
 44. El-Shafei HM. Some heavy metals concentration in water, muscles and gills of tilapia niloticus as biological indicator of Manzala Lake pollution. *J Aquacul Res Develop.* 2015;6(9):2–5.

45. Ahmed MK, Baki MA, Islam MS, et al. Human health risk assessment of heavy metals in tropical fish and shellfish collected from the river Buriganga, Bangladesh. *Environ Sci Pollut Res*. 2015;22:15880–15890. <https://doi.org/10.1007/s11356-015-4813-z>
46. Hussain B, Sultana T, Sultana S, et al. First report on fish cysteine as a biomarker of contamination in the River Chenab, Pakistan. *Environ Sci Pollut Res*. 2016;23(15):15495–15503. <https://doi.org/10.1007/s11356-016-6711-4>
47. Mulk S, Korai AL, Azizullah A, Shahi L, Khattak MN. Marble industry effluents cause an increased bioaccumulation of heavy metals in Mahaseer (*Tor putitora*) in Barandu River, district Buner, Pakistan. *Environ Sci Pollut Res Int*. 2017;24(29):23039–23056. <https://doi.org/10.1007/s11356-017-9921-5>
48. Azizullah A, Khattak MN, Richter P, Häder DP. Water pollution in Pakistan and its impact on public health—a review. *Environ Int*. 2011;37(2):479–497. <https://doi.org/10.1016/j.envint.2010.10.007>
49. Alam I, Khattak MN, Mulk S, Dawar FU, Shahi L, Ihsanullah I. Heavy metals assessment in water, sediments, algae and two fish species from river Swat, Pakistan. *Bull Environ Contamin Toxicol*. 2020;105:546–552. <https://doi.org/10.1007/s00128-020-02981-z>
50. Khan B, Khan H, Muhammad S, Khan T. Heavy metals concentration trends in three fish species from Shah Alam River (Khyber Pakhtunkhwa Province, Pakistan). *J Nat Environ Sci*. 2012;3(1):1–8.
51. Chatta AM, Khan MN, Hadyat I, Ali A, Naqvi SA. Detection of heavy metals (cadmium, lead and chromium) in farmed carp fish species, marketed at Lahore, Pakistan: a serious health concern for the consumers. *Int J Biosci*. 2017;10(4):199–211. <http://dx.doi.org/10.12692/ijb/10.4.199-211>
52. Ihtisham-Ur-Rahman IA, Khan A, Ahmad W, et al. Heavy metals (Lead and Cadmium) concentration in different organs of mahseer (*Tor putitora*) of river Indus at Swabi, KPK, Pakistan. *Pure Appl Biol*. 2020;9(4):2158–2166. <http://dx.doi.org/10.19045/bspab.2020.90230>
53. Yousafzai AM, Khan AR, Shakoori AR. Heavy metal pollution in River Kabul affecting the inhabitant fish population. *Pak J Zool*. 2008;40(5):331–339.

54. Khalil A, Jamil A, Khan T. Assessment of heavy metal contamination and human health risk with oxidative stress in fish (*Cyprinus carpio*) from Shahpur Dam, Fateh Jang, Pakistan. *Arab J Geosci.* 2020;13:1–10. <https://doi.org/10.1007/s12517-020-05933-3>
55. Ali H, Ali W, Ullah K, Akbar F, Khan H. Assessment of Cu and Zn in water, sediments and in the carnivorous fish, *Channa gachua* from River Swat and River Barandu, Malakand Division, Pakistan. *Iran J Sci Technl Transac.* 2019;43(1):773–783. <https://doi.org/10.1007/s40995-018-0615-8>
56. Shah D, Karibayev M, Adotey EK, Torkmahalleh MA. Impact of volatile organic compounds on chromium containing atmospheric particulate: insights from molecular dynamics simulations. *Sci Rep.* 2020;10(1):e17387. <https://doi.org/10.1038/s41598-020-74522-x>
57. Idrees M. Analysis and human health risk from selected heavy metals in water, sediments and freshwater fish (*Labeo Rohia*, *Cyprinus carpio*, *glypthothorax Punjabensis*) collected from three rivers in district Charsada, Khyber-Pakhtonkhuwa, Pakistan. *Carpath J Earth Environ Sci.* 2017;12(2):641–648.
58. Naeem S, Ashraf M, Babar ME, Zahoor S, Ali S. The effects of some heavy metals on some fish species. *Environ Sci Pollut Res.* 2021;28(20):25566–25578. <https://doi.org/10.1007/s11356-021-12385-z>
59. Bano Z, Abdullah S, Ahmad W, Zia MA, Hassan W. Assessment of heavy metals and antioxidant enzyme in different organs of fish from farm, hatchery and Indus river of Pakistan. *Pak J Zool.* 2017;49(6):2227–2233.
60. Mohamed AA, El-Houseiny W, Abd Elhakeem EM, Ebraheim LL, Ahmed AI, Abd El-Hakim YM. Effect of hexavalent chromium exposure on the liver and kidney tissues related to the expression of CYP450 and GST genes of *Oreochromis niloticus* fish: Role of curcumin supplemented diet. *Ecotoxicol Environ Saf.* 2020;188:e109890. <https://doi.org/10.1016/j.ecoenv.2019.109890>
61. Waheed S, Kamal A, Malik RN. Human health risk from organ-specific accumulation of toxic metals and response of antioxidants in edible fish

- species from Chenab River, Pakistan. *Environ Sci Pollut Res.* 2014;21:4409–4417. <https://doi.org/10.1007/s11356-013-2385-3>
62. Hamid A, Khan MU, Yaqoob J, et al. Assessment of mercury load in river Ravi, urban sewage streams of Lahore Pakistan and its impact on the oxidative stress of exposed fish. *J Biodivers Environ Sci.* 2016;8(4):63–72.
 63. Iqbal A, Tabinda AB, Yasar A, Mahfooz Y. Heavy metal uptake and toxicity in tissues of commercially important freshwater fish (*Labeo rohita* and *Wallago attu*) from the Indus River, Pakistan. *Pol J Environ Stud.* 2017;26(3):627–633. <https://doi.org/10.15244/pjoes/66850>
 64. Jabeen F, Chaudhry AS. Monitoring trace metals in different tissues of *Cyprinus carpio* from the Indus River in Pakistan. *Environ Monitor Assess.* 2010;170:645–656. <https://doi.org/10.1007/s10661-009-1263-4>
 65. Yousafzai AM, Ullah F, Bari F, et al. Bioaccumulation of Some Heavy Metals: Analysis and Comparison of *Cyprinus carpio* and *Labeo rohita* from Sardaryab, Khyber Pakhtunkhwa. *BioMed Res Int.* 2017;2017:e5801432. <https://doi.org/10.1155/2017/5801432>
 66. Munir MA, Khan B, Mian IA, et al. Assessment of Hg accumulation in fish and scalp hair in fishing communities along river Swat, Pakistan. *Environ Sci Pollut Res.* 2021;28:67159–67166. <https://doi.org/10.1007/s11356-021-15348-6>
 67. Ahmed Q, Bat L, Öztekin A, Ali QM, Ghory FS, Yousuf F. Metals levels in *Sarda orientalis* collected from the commercial landings of Karachi Fish Harbor, Pakistan (northern Arabian Sea) and assessment of likely health risks to the consumers. *Int J Rapid Commun.* 2023;56(2):73–84. <https://doi.org/10.1080/00387010.2023.2165506>
 68. Chatha AMM, Naz S, Mansouri B, Nawaz A. Accumulation and human health risk assessment of trace elements in two fish species, *Cirrhinus mrigala* and *Oreochromis niloticus*, at Tarukri Drain, District Rahimyar Khan, Punjab, Pakistan. *Environ Sci Pollut Res.* 2023;30:56522–56533. <https://doi.org/10.1007/s11356-023-26337-2>
 69. Saeed F, Iqbal KJ, Atique U, et al. Toxic trace metals assessment in selected organs of edible fish species, sediment and water in Head Punjnad, Punjab, Pakistan. *Punjab Univ J Zool.* 2020;35(1):43–50. <https://dx.doi.org/10.17582/journal.pujz/2020.35.1.43.50>